Energy Redistribution with Controllable Binary State Latch Element

Chiang-Kai Chu

Thesis submitted to the Faculty of the
Virginia Polytechnic Institute and State University
in partial fulfillment of the requirements for the degree of

Master of Science
in
Mechanical Engineering

Steve C. Southward, Chair
Andrew J. Kurdila
Lei Zuo

May 9, 2017
Blacksburg, Virginia

Keywords: Variable Structure System, Vibration control, Energy harvesting, Semi-active device, Smart Spring, Multi-agent device, Energy redistribution

Energy Redistribution with Controllable Binary State Latch Element

Chiang-Kai Chu

(ABSTRACT)

An application of binary state latch device with proper real-time control algorithm for energy redistribution application is introduced in this thesis. Unlike traditional tuned vibration absorber, the latch device can be viewed as variable semi-active dampers such as magnetorheological (MR) and piezoelectric friction dampers. The distinct difference between other semi-active dampers and our latch device is that other semi-active dampers can provide continuous resistance according to the amount of input current, however, the binary latch device can only provide two different values of resistance - either the maximum or no resistance at all. This property brings the latch possibly having higher maximum and minimum ratio of resistance than MR dampers. As for the operating structure, the mechanism of latch element is nearly the same as the piezoelectric friction dampers which the resistance force is provided according to the normal force acting on two rough plates. Nonetheless, because of the characteristic of the binary states output of the latch element, this make it very different from the ordinary variable dampers. Since it is either being turned on or turned off, a novel control law is required for shifting energy. Also, because of the simplicity of the binary states output, it is very accessible to implement the controller on Field Programmable Gate Array (FPGA). With this accessibility, it is promising to apply plenty of latch elements in the same time for large scale application, such as multi-agent networks. In this thesis, an energy-based analytic solution is proposed to illustrate the universal latch-off condition. And a latch-on condition under ideal situations is discussed. At the end, a control law under nonideal condition is being suggested for real-time periodically excited system. We found that energy redistribution is achievable by using the proper control law under fairly broad conditions.

Energy Redistribution with Controllable Binary State Latch Element

Chiang-Kai Chu

(GENERAL AUDIENCE ABSTRACT)

A simple dynamic structure with a latch element device is introduced in this thesis. We found that energy redistribution is achievable by using a particular control law under specific condition. A energy-based analytic solution is introduced to illustrate the strategy of the energy transfer process under ideal condition. At the end of the thesis, we proposed non-single switch algorithm for real-time application. In this thesis, we found that energy redistribution is possible for this one dimentional structure. The latch devices can be implemented into two dimensional networks. If enery redistrbution is also possible for two dimentional multi-agent networks, it is promising to use it to do not only energy redirection to protect target from vibration but we can also accumulate the energy for energy harvesting.

Acknowledgments

I would first like to thank my advisor Dr. Steve Southward. The door to Prof. Southward office was always open whenever I ran into a trouble about my research or writing or even the presentation for defense. He consistently allowed this paper to be my own work, but steered me in the right direction whenever he thought I needed it.

Also, I must express my profound gratitude to my parents , to my girlfriend and to my friends for providing me with unfailing support and continuous encouragement throughout my years of study and through the process of researching. This accomplishment would not have been possible without them. Thank you.

Author
Chiang-Kai Chu

Contents

List of Figures

List of Tables

Chapter 1

Introduction

1.1 Motivation

Vibration reduction techniques are being widely applied to areas such as transportation vehicles, semiconductor fabrication plant, or skyscrapers where places need to be comfortable and safe for human beings, or performing high precision machining. The stability of these circumstances need to be achieved even under extreme environment conditions. In those situation, fixed-parameter vibration absorber might not carry out effective vibration reducing results. Therefore, variable semi-active control devices like magnetorheological damper ([23], [15], [16]), piezoelectric friction damper ([11], [12], [13], [14]) are being developed to overcome such difficulties. Magnetorheological (MR) dampers is a application of magnetorheological fluid which is a suspension of small magnetic particles. The crucial behavior of MR fluid is the ability to change from free-flowing, providing viscous resistance, to viscoelastic solid which have yield strength controlled by the density of electric or magnetic field within fractions of seconds. The ratio of maximum to minimum force a MR damper (α) can provide represent the operating range of the damper. The higher operating range means that the damper is more flexible to be implemented under various conditions. This flexibility motivates us to develop a new kind of device which is able to provide very large maximum to minimum ratio of the output force. Unlike MR dampers still have viscous resistance even without applying it with magnetic field, there is nearly no resistance within our binary state latch when the latch is in its off state. In consequence, without having resistance in the off state, the ratio α can be extremely large. For example, in fig.(1.1), the ratio α_{Latch} is much greater than α_{MR}.

$$\alpha = \frac{Max.friction}{min.friction} \tag{1.1}$$

(a) Output resistance of MR damper (b) Output resistance of latch element

Figure 1.1: Different behavior of Force/velocity response between MR damper and latch element

$$\begin{cases} \alpha_{MR} & = \frac{4}{1.5} \cong 2.67 \\ \alpha_{Latch} & = \frac{4}{0} \rightarrow \infty \end{cases} \tag{1.2}$$

Furthermore, with the fearture of zero resistance while latch is off, the energy is more likely to be preserved in the system instead of being dissipated. Since the energy can be preserved, it provides a possibility to retain more energy and redirect it for further purpose. In this thesis, we focus on developing a control law acting on a binary state latch element to make desired energy redirection in the system.

1.2 Literature review

1.2.1 Vibration absorber

Due to the unpredictable characteristic of earthquakes, structural control has been considered one of the most effective strategies to protect buildings from intense dynamic events in recent years [29]. Structural control strategies can be catergorized into four class: passive, semi-active, active and hybrid control. Because the passive control strategy doesn't need any external power source, it have already been widely implemented in various engineering fields. However, the application of passive systems are limited by lacking of the ablility to adapt to structural changes or different enviornmental conditions. On the other hand, active systems are able to adapt under different conditions. But they require significant amount of energy to supply large enough control forces. Even worse, the stability of active systems is not gurranteed. To overcome the drawbacks of both control systems, semi-active control systems have been introduced. Semi-active control devices do not require large energy supply

but they are adaptible to different external inputs. Since there is no direct energy flow into the structural system, semi-active control device do not have the potential to destabilize the system.

Magnetorheological damper

Magnetorheological (MR) damper is one of the promising device for semi-active control [24]. The MR damper is filled with magnetorheological fluid and the amount of resistance in the damper is operated by magnetic field applied on the fluid. When the fluid is brought into a magnetic field, the metal particles inside the fluid interact with the field and create resistance by making the fluid stiff.

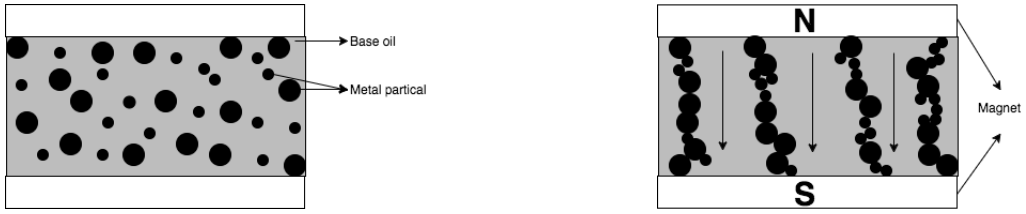

(a) No magnetic field applied

(b) Magnetic field applied

Figure 1.2: Configuration of MR damper

The main advantages of MR dampers are that they need very less control power, having simple construction, fast response to control signal and very few moving parts. The main control strategy is to adjust the maximum forces of the damper provided. The maximum saturation force generated by a MR damper is proportional to the density of the magnetic field. By varying the current in the induction coil, we can control the density of the field. However, MR dampers still provide resistance force even without magnetic field because of the viscosity of the fluid inside the damper.

Vibration control for piezoelectric material

Because of the similarity structure of latch element and friction damper, we introduce the mechanism of the friction damper.

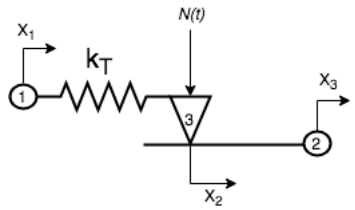

Figure 1.3: Schemetic of friction damper

In fig.(1.3), the model have three nodes. Node 1 and 2 are the connecting points, and node 3 is the place where friction occurs sometimes being called "slider". The force between nodes 1 and 2 is given as,

$$F_f = \begin{cases} k_T(x_2 - x_1) & \text{if } |k_T(x_2 - x_1)| \leq \mu N \\ \mu N & \text{otherwise} \end{cases} \tag{1.3}$$

Eq. (1.3) show the proportionality between the force F_f and the relative displacement. After the F_f reaches the friction maximum μN, the damper acts as a ordinary spring with coefficient k_T. The Harmonic Balance Method (HBM) ([37], [38]) is one of the methodology used to develop the control algorithm of a friction damper to avoid the system being excited harmonically. One other often used control laws for friction damper is Maximum Energy Dissipation (MED) [39]. The core concept of MED is to dissipate energy away by making the damper create a force while the system is deviating from its static equilibrium position. Otherwise, the system moves toward to its equilibrium position freely. The relationship between exterting force and relative displacement is being addresed in eq.(1.4).

$$F_{MED}(\theta) = \begin{cases} k_T(x_2 - x_1) & \text{for sign}(x \times \dot{x}) > 0 \\ 0 & \text{for sign}(x \times \dot{x}) \leq 0 \end{cases} \tag{1.4}$$

To assess the effectiveness of different control methodologies applied on friction dampers, the qualititive levels of the required normal force and the resulting attenuation are being evaluated. According to Table 1.1, the best performance for a friction damper was achieved with low normal force and high level of attenuation. In fact, this table could be used to classify any semi-active vibration absorbing device. Due to the low energy consuming and high attenuation characteristic, it also explained the reason that semi-active dampers becomes more and more attractive in recent year.

Table 1.1: Table of the merit of the dampers performance.

		Normal Force	
		Low	High
Attenuation	Low	Fair	Poor
	High	Good	Acceptable

Piezoelectric device with state switch control

The other important vibration control method using piezoelectric device is the state switch control method implemented on a shunt circuit. The basic application of the shunt circuit is the passive shunt damping. The main characteristic of its mechanism is the transferation of mechanical strain energy into electrical energy via Piezoelectricity(PZT)-based transducers. The structural vibration is damped through dissipating into heat in the shunt piezoelectric circuit. For a purely passive shunt it is stable since no external power supply. However, it is not effective to do large amplitude vibration suppresion. To overcome the disadvantage of pure passive shunts, the concept of a switch leads to various switching techniques.

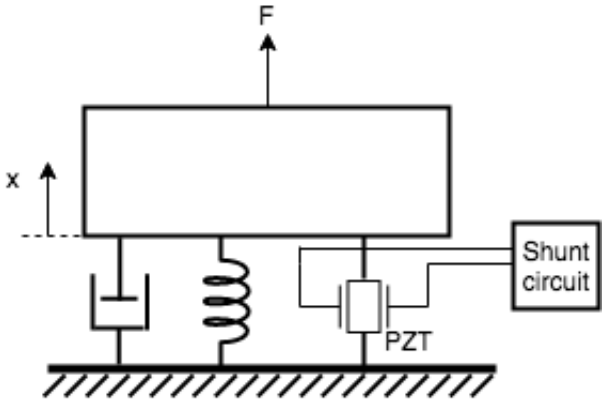

Figure 1.4: Schematic of piezoelectric devices

1. State switch: The first concept of state switching is used by Larson [33] to develop a high-stroke acoustic source at a wide frequency rage. Another application of state switching technique for vibration control is used by Clark [34]. By adjusting the stiffness (equivalent to the resistance in electrical domain) of the system using the open or short-circuit states of PZT fig.(1.5). He short the circuit while the system is moving toward the equilibrium

to low-stiffness state; On the contrary, the system being switched to open-circuit (high-stiffness state) if the system is moving away. This switching condition is universal for all kinds of switch control techniques. The differences between the techniques are the electrical components used in the circuit.

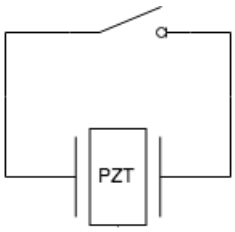

Figure 1.5: Schematic of state switch

2. Synchronized switched damping (SSD) on a resistive shunt (SSDS): As in fig.(1.6), a resistance is being connected in the circuit. The conclusion made in [35] was that the state switch and SSDS had higher performance than purely passive case and could be an alternative to active control in certain frequency ranges.

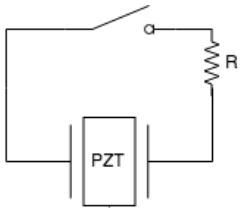

Figure 1.6: Schematic of synchronized switched damping on a resistive shunt

3. Synchronized switched damping on an inductive shunt (SSDI): In [36], Corr and Clark compared the performance of state switching and SSDI with a tuned inductive shunt. It had been shown that both SSDI and tuned inductive shunt technique had better performance than the state switching technique and less susceptible to system changes than the inductive shunt.

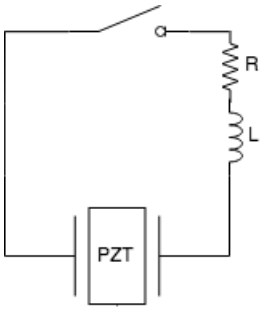

Figure 1.7: Schematic of synchronized switched damping on an inductive shunt

Application of PZ friction damper

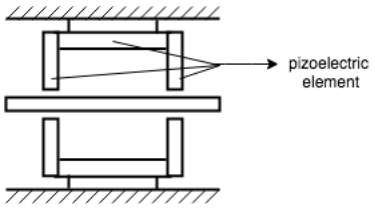

Figure 1.8: Schematic of inchworm motor

Not only used for vibration control, piezoeletric device had another application[40], such as the ultrasonic motors in camera lenses. The motors is made of three parts of piezoelectric elements, and two of them have same mechanisms as a PZ friction dampers. By controlling the voltage pass through the pizoelectric elements, the lenghth of it changed. The mechanism of inchworm motors can be illustrate into six repeating cycles in fig.(1.8).

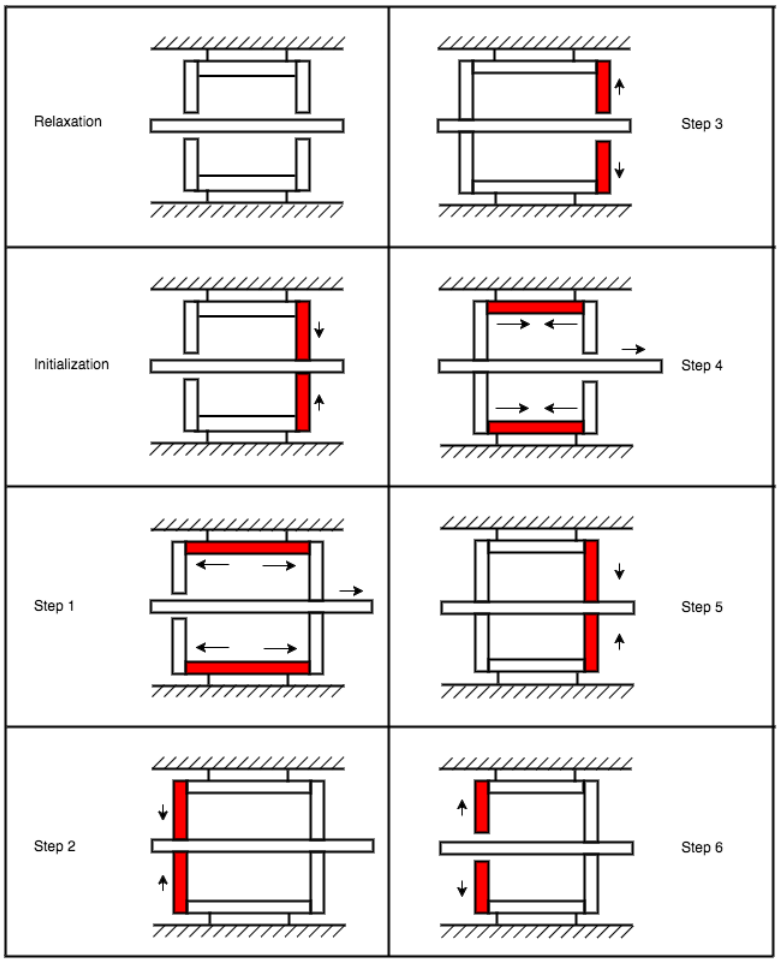

Figure 1.9: Working process of inchworm motor

Relaxation step. All piezo elements are in relaxation.

Initialization step. Extension of the right side clutch piezo elements.

Step 1. Extension of the lateral piezo elements.

Step 2. Extension of the left side clutch piezo elements.

Step 3. Relaxation of the right side clutch piezo elements.

Step 4. Relaxation of the lateral piezo elements.

Step 5. Extension of the right side clutch piezo elements.

Step 6. Relaxation of the left side clutch piezo elements.

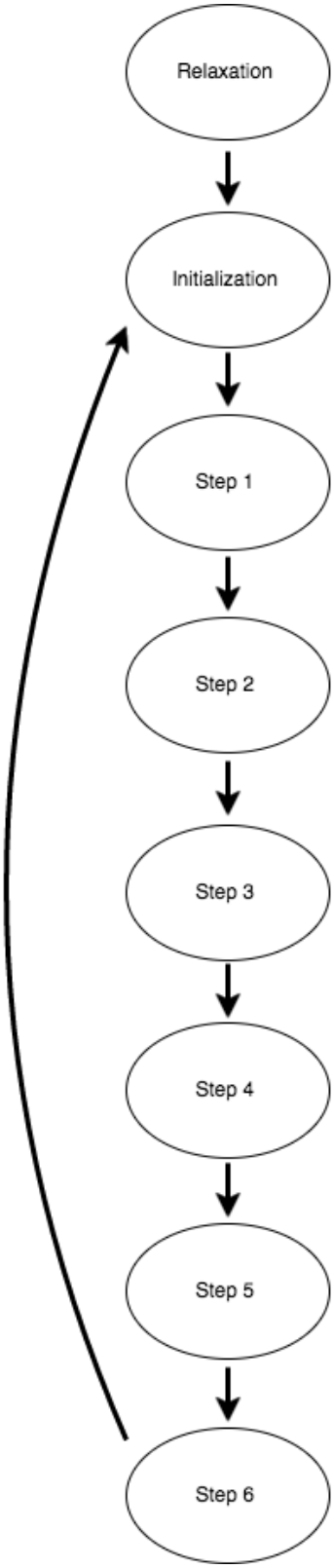

Figure 1.10: Flow chart of working process for inchworm motors

Smart Spring devices

The Smart Spring is a patented concept [31] constructed by an actively variable friction device using piezoelectric materials to vary the stiffness and damping of dynamic systems. The mechanism is shown in fig.(1.11). The Smart Spring is placed between the perturbation source and the target section. By controlling the input voltage to the piezoelectric element, the normal force $N(t)$ is being generated to create the friction force $F_f(t)$ between the element and the sleeves. Furthermore, while the voltage is being applied, the spring K_2 starts playing a part in the dynamics. With this ability to control the friction and impedance, the Smart Spring device is able to vary the combinations of stiffness and damping.

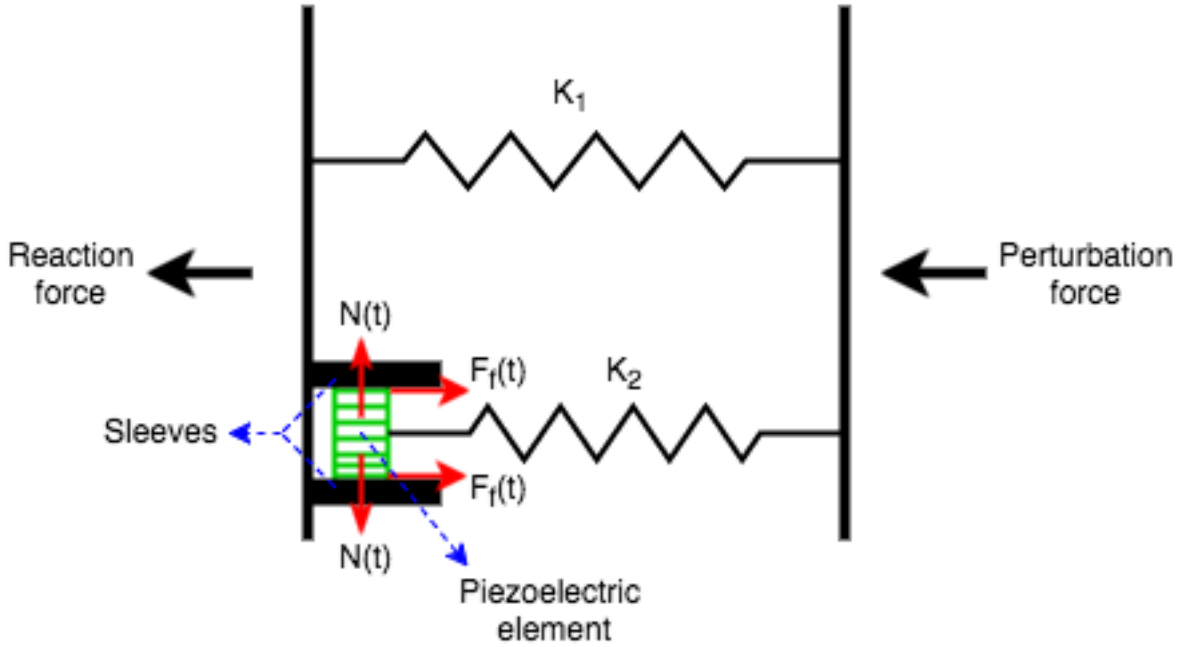

Figure 1.11: Schematic of Smart Spring device

The main advantage of the Smart Spring is its indirect process of vibration suppression. The piezoelectric actuator controllably engages the spring to affect the impedance of a structure. Moreover, the piezoelectric actuator are able to generate sufficient forces with low voltage, making the Smart Spring more feasible to be implemented. One of the application of Smart Spring device is the vibration control of helicopter blades [32]. In this application, Smart Spring device is an active tunable vibration absorber using Individual Blade Control (IBC) techniques to alter the structural impedance. The device is able to overcome the obstacle for ordinary piezoelectric actuators, reducing significant structural vibration on the blades.

1.2.2 Variable structure system

Nonlinear dynamical systems have been frequently investigated in recent years due to its complexity and the possibility to have additional useful properties. Since the system in the reality are always nonlinear overall and only behave linearly on a relatively small working range under strict requirements, it is more precise to model real systems in nonlinear system structure. Variable Structure System (VSS) is one kind of interesting nonlinear system which involves switching control input, allowed the system to change its structure. The concept of VSS appeared in late fifties in various researches ([17], [18], [19], [20], [21]). The paper published by S. Emel'yanov ([1]), mentioned that by altering the structure in the progress of control process, the system could gained the properties that are not possessed by any of the subsystem. In a review article written by S.V.Emel'yanov ([22]), he described the beginning discovery of VSS. The problem being investigated by his research group ran into difficulties that negative feedback gains could not ensure large enough control signal to suppress finite additive or parametric disturbances. The problem was solved by applying both negative and positve feedback and resulted in an unstable structure. With this instability, even small feedback coefficients allow high enough control signal to supress noise and other uncertain factors. He discovered that stability in the large could be achieved by applying feedback to alter the system structure between an unstable system and a stable system. It is the main concept in the VSS theory, and also known as the principle of structure variability afterwards. The advantages of VSS are the uncharacteristic of linear, adaptive, or relay systems, and they have brought lot of attention to this topic even now.

1.2.3 Mechanical energy harvesting

Coal, petroleum are the essential energy sources to our daily life. However, the amounts of those resources are limited on earth. We dont have access to non-renewable energy forever. Thus, it becomes crucial acquire sustainable energy. As we know, energy exists in our surroundings in many kinds of forms, such as light, wind, temperature difference and vibrations. However, the scale of energy of these sources is often too small to provide sufficient power for practical purpose. As a result, these kinds of energy usually being regard to be useless or wasted, until energy harvesting techniques being recently investigated. In order to do effective energy harvesting, devices built for this purpose need to be efficient for capturing, accumulating, storing ambient energy. The development of renewable energy harvesting technologies have leaded to the development of self-powered system. Self-powered systems possessed the features that it only need minimum maintenance, and thus it can be deployed in inaccessible locations.

In some situation where solar, thermal, wind or other form of renewable energy is not suitable, mechanical energy is thought to be the most promising energy sources because of its abundance presence in daily life. Mechanical energy is produced related to vibrating structure, motion of living beings, flow induced vibration and noise. There are multiple ways to

harvest mechanical energy, like using piezoelectric material, electromagnetic or electrostatic transducer convert the mechanical energy into electrical energy.

Table 1.2: Comparison of vibrational energy harvesting technologies.

Mechanism	Energy density	Current size	Drawbacks
Piezoelectric	$35.4mJ/cm^3$	Macro	Low output voltage
Electromagnetic	$24.8mJ/cm^3$	Macro	Very low output voltage
Electrostatic	$4mJ/cm^3$	Integrated	Need for initial charge source

Piezoelectric (PZ) materials : Piezoelectricity is the electric charge accumulates in certain material, such as crystals and certain ceramics, caused by applied mechaincal stress. The mechanical stress induce charge seperation in the material and generates a surface charge on the material, producing an electrical field. The electric potential difference across this field is proportional to the mechanical strains applied to the material. If the mechanical load is oscillating, the PZ device can provide alternating current power source (AC).

Electromagnetic device : The device is simply a application of Faraday's law. By using a vibrating object attached with a coil passing through a static magnetic field to induce electric potential difference in the coil, we are able to harvest the energy from the voltage drop. If the voltage drop is too low, we can use transformers to amplified it to get proper voltage difference.

Electrostatic (capacitive) systems : We use a variable capacitor as an electromechanical transducer. The vibration provides variations to the distance between two plates which are initially charged. If we keep the charge on the plates constant, the energy of the electric field stored in the capacitor will varied with this distance. Resulting in a flow of current in the coil. One of the main advantages of capacitive energy harvesting systems is that they can be easily implemented on ICs.

1.3 Thesis outline

In this thesis, we are introducing a vibration redirection device which is capable to transfer energy within the system. In chapter one, we show the basic system configuration, and explain the properties of the latch element – the critical element we used for vibration absorbing in this thesis. In chapter three, we derive and show the existence of an analytic solution for a single switch latch system under ideal conditions, based on energy conservation aspect. Nevertheless, in chapter four, we find that the existence of the solution is not unique neither for the case that the system is excited by external force or not being excited. We show the property of uniqueness by a optimization technique that simply shows numerous

of final cost which derived from every different possible control process applying on the latch element. Chapter five, we explore the condition for the excited system which can be a guidline for the controller to turn on the latch. Next in chapter six, we implement the result concluded from chapter five on real-time control simulations to see if the control law is valid. Finally, conclusions and promising future work is being addressed in chapter 7.

Chapter 2

Dynamics system model

2.1 Two mass dynamics system with single latch

The system model being examined in this thesis is a typical second-order spring-mass-damper system inseries with a latch device. While the latch is off, each of the masses belongs to a separate subsystem. Subsystem M_1 is composed of spring k_1 and mass M_1, and subsystem M_2 is composed of a spring k_2, a damper b_2 and mass M_2. The external force is acting on M_2. By turning the latch element on, we connect two masses together. After this connection, no relative motions exist between M_1 and M_2 under ideal condition. For simplicity we assumed that $M_1 = M_2$ in our system model.

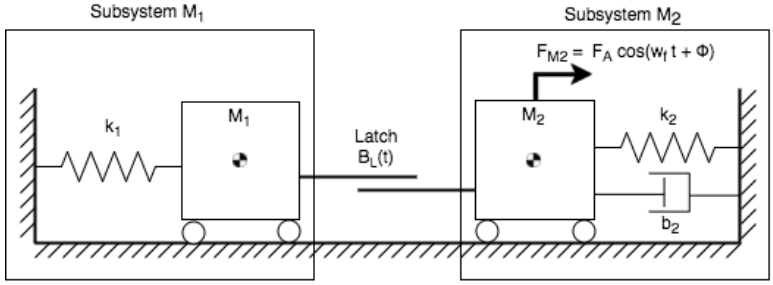

Figure 2.1: Complete dynamic system model

Here, we introduce symbols used to describe the system.

$$w_{M1} : Natural\ frequency\ of\ M_1$$
$$w_{M2} : Natural\ frequency\ of\ M_2$$
$$F_A : Amplitude\ of\ optional\ external\ force$$
$$w_f : Frequency\ of\ external\ force$$
$$\phi : Phase\ angle\ of\ external\ force$$

2.2 Detail description of latch element

The schematic of latch device is shown in fig.(2.2). It is constructed by two parallel plates. Node N1 and N2 are the connecting point to the external. Node N3 is place where clench occurs providing friction to prevent relative motion between N1 and N2. The response of the coefficiet of a latch device is being modeled as a equivalent variable damper with a very large damping coefficient. $B_L(t)$.

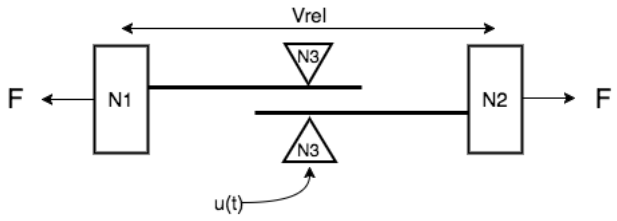

Figure 2.2: Conceptual mechanism of latch device

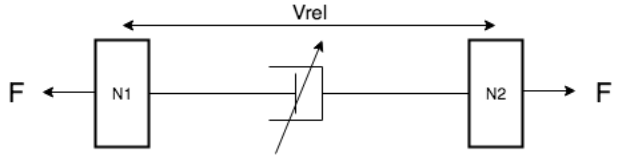

Figure 2.3: Equivalent model for latch device

The equation for force to relative velocity relation of this equivalent damper is,

$$F = B_L(u)V_{rel} \tag{2.1}$$

As for the damping coefficient $B_L(u)$, we use this first order differential equation to describe it,

$$\begin{aligned} B_L(u) &= B_{Max}\left(\frac{1}{\tau s+1}\right)u \\ B_L(\tau s+1) &= B_{Max}u \\ \tau\dot{B}_L(t) + B_L(t) &= B_{Max}u \\ \dot{B}_L(t) &= \frac{B_{Max}u - B_L(t)}{\tau} \end{aligned} \tag{2.2}$$

We can control the damping coefficient of the latch by the control $u(t)$. Once the control signal is on, the latch coefficient start increasing to reach its maximum according to the equation.(2.2), and remain in its maximum until receiving turn-off control signal. The friction force exert from latch element is propotion to the normal force acting to the interacting

surface. Since the normal force is not possible to reach its maximum instantaneously as the control signal being turned on, there always exists a time delay before the force increasing to its maximum. To make the latch behave more realistic, we model the response of latch with a time delay. The response for latch being turned off is also modeled by equation.(2.2). The reaction of the latch response to the control signal is shown in the fig.(2.4)

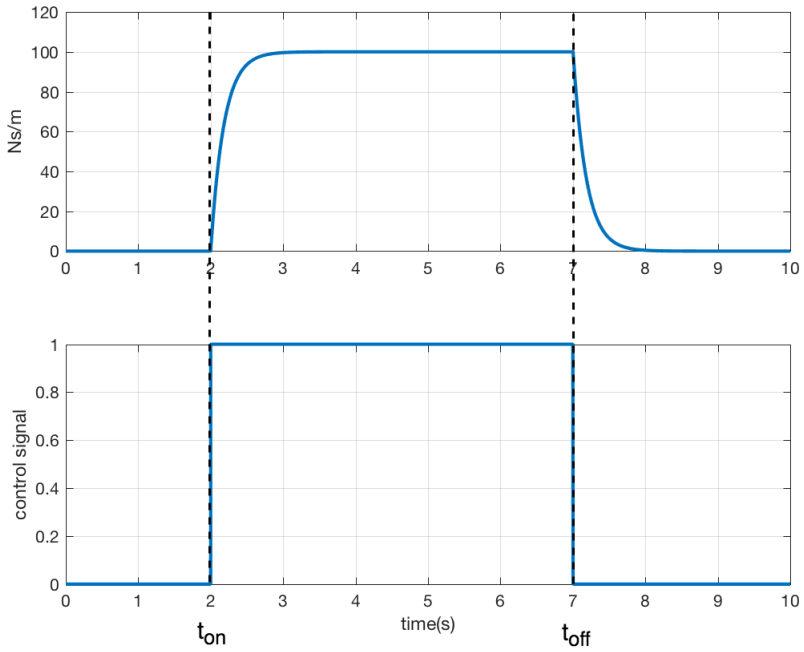

Figure 2.4: Latch coefficient response

Chapter 3

Existence of single switch control

In this chapter we are going to use the system without dampers and external force to illustrate the existence of the single switch control algorithm under ideal condition. The fig.(3.1) is the system model we use.

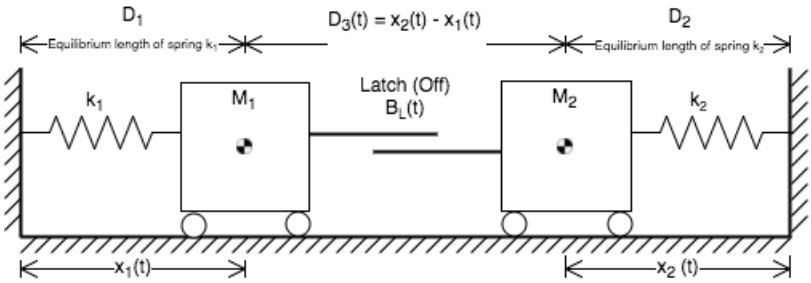

Figure 3.1: System without dampers and disturbation

3.1 Define cost function and control event

The goal of our task is minimizing the energy in M_1. Because there is no resistance except from the turn-on latch element, the cost will remain the same after the single switch control finished. We obtain cost by combining the kinetic and potenial energy in M_1 together after the control process is finished. In order to explicitly shows the effectivity of the control process, we evaluate the normalized cost by dividing the cost with the initial energy in M_1.

$$\begin{aligned} J &= \frac{Final\ Enery\ in\ M_1}{Initial\ Energy\ in\ M_1} \\ &= \frac{(M_1 v_1^2 + K_1 x_1^2)}{(M_1 v_{10}^2 + K_1 x_{10}^2)} \end{aligned} \tag{3.1}$$

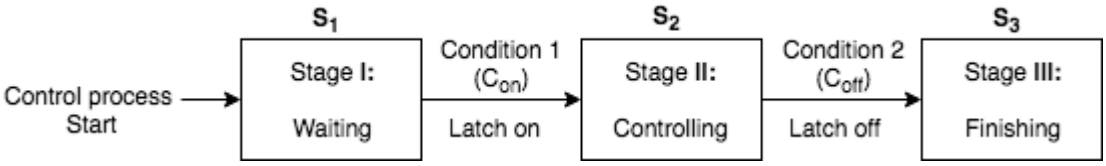

Figure 3.2: Single switch control process

Since we only consider a single switch on/off event in this paper, we thus can separate the control process into three stages. Those are, waiting, controlling, ending. Where waiting state represents the part of process prior to the latch being turned on, and the controlling process is the period when the latch is on. For the last stage, ending state means the process after the latch is off. To facilitate what are the conditions for triggering the controller to go into next stage, we illustrate the process backward in time. In the last stage of the control event (Stage III), our goal is to diminish the vibrations of M_1. From energy perspective, the energy in M_1 must close to or equal to zero to make M_1 stop moving. To achieve this, the velocity of M_1 and the distance between current position of M_1 and the original equilibrium position of M_1 also have to equal to zero to prevent M_1 bouncing back to the equilibrium of subsystem M_1 creating vibration after two subsystems are separated. Thus, the condition of zero velocity and zero displacement triggers the controller in Stage II to go into the last stage. We called this condition C_{off}, which makes the latch to turn-off. It can also be thought that condition C_{off} to be zero kinectinc energy and zero potential energy in M_1 respect to the subsystem of M_1. Next, the question need to be answer is what is the conditions C_{on}, making the controller from first stage to go into the second stage. In other words, what is the approriate condition to turn on the latch. In the next section, we are going to demonstrate a analytic solution for this problem with a zero-input system without external excitation.

3.2 Analytic ideal solution

3.2.1 Limited conditions and assumptions

Assumption 1 In reality, there always exists a time delay before the latch is fully turned on or fully turned off. With this time delay, it is hard to get the analytic solution. For simplicity, we are going to use the assumption that the effect of this time delay is negligible. So time constant for an ideal latch device need to be very small, and also we don't want any relative motion between two ends of the latch, so we say the maximum coefficient (B_{Max}) for an ideal latch should be,

$$\begin{cases} B_{Max} \geq 6000 & (N\ m/s) \\ \tau \leq 10^{-7} & (s) \end{cases}$$

The ideal latch coefficient we assumed is shown in fig.(3.3).

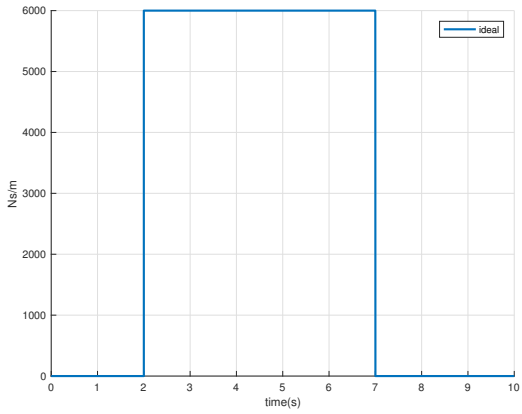

Figure 3.3: Damping coefficient of an ideal latch

Assumption 2 The previous assumption lead us to apply theory of inelastic collision to describe the system when the latch is being turned on. If the latch being turned on instantaneously without time delay, this process can be seen as a perfect inelastic collision between M_1 and M_2. If the system is having a perfect inelastic collision, the kinectic energy lost by bonding the two bodies together. However, the momentum of the system is conserved. By the conservation of momentum we know that,

$$\begin{aligned} M_1 v_1 + M_2 v_2 &= (M_1 + M_2) V_{inelastic} \\ V_{inelastic} &= \frac{M_1 v_1 + M_2 v_2}{M_1 + M_2} \end{aligned} \tag{3.2}$$

From 3.2, the velocity of M_1 and M_2 after the collision is accessible for further calculation.

Limited conditions If subsystems M_1 and M_2 have the same natural frequency, and also being given the same initial conditon, our control method is not possible to be implemented.

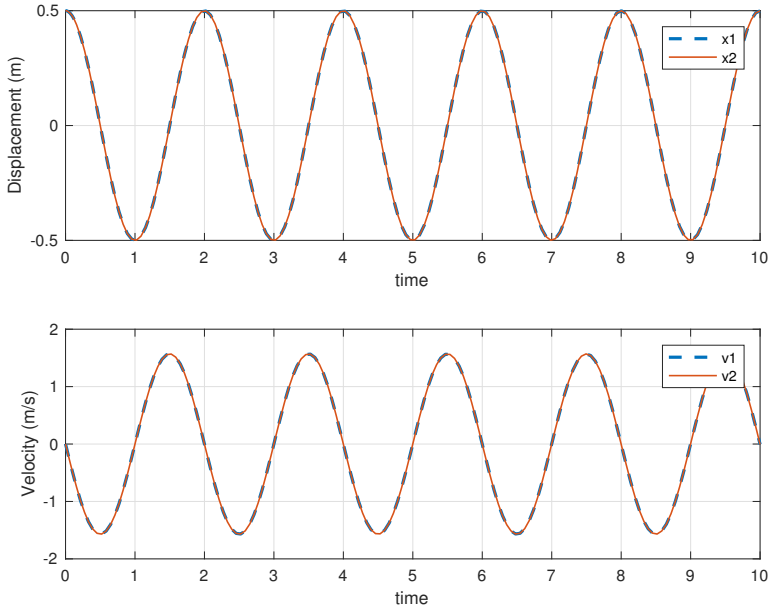

Figure 3.4: The case fail to apply control

In fig.(3.4), Since M_1 and M_2 have the same phase and amplitude, the distance between them is always a constant. According to our following analysis, the control law is not applicable in this situation.

3.2.2 Ideal analytic conditions at t_{on} and t_{off}

Our strategy to solve zero-input system comes from observations of simple harmonic motion systems. Assuming that there is a SDOF system with one mass element connected with spring between the boundary and the mass fig.(3.5a).

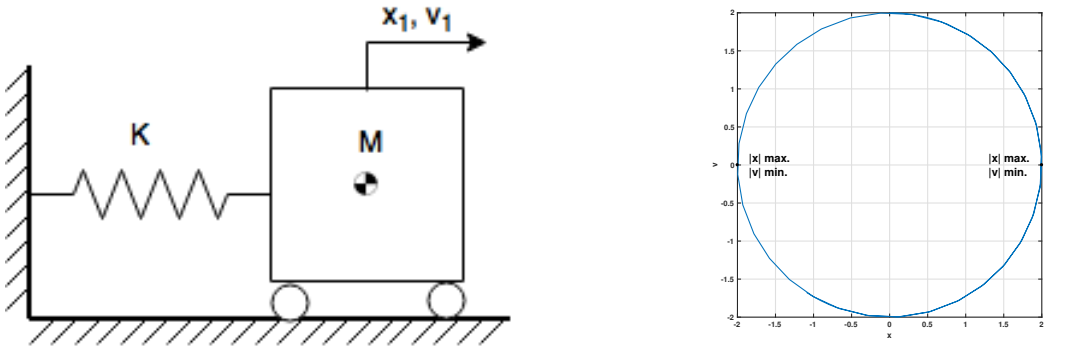

(a) Diagram of SHM system

(b) Phase plot of SHM system

Figure 3.5: Simple harmonic system

By observing the phase portrait in fig.(3.5b), the system have zero velocity while the mass is at its farthest position from the equilibrium. According to our design of control process, we should turn off the latch while M_1 have zero velocity at the original equilibrium of subsystem M_1. That is, turn off the latch element when the subsystem M_1 having zero kinectic and potential energy. By observing the SHM system, we know that M_1 has zero kinectic energy while it reaches the farthest position it can achieve. The remaining condition to turn off the latch is to make M_1 possess a zero potential energy with respect to the separated subsystem M_1.

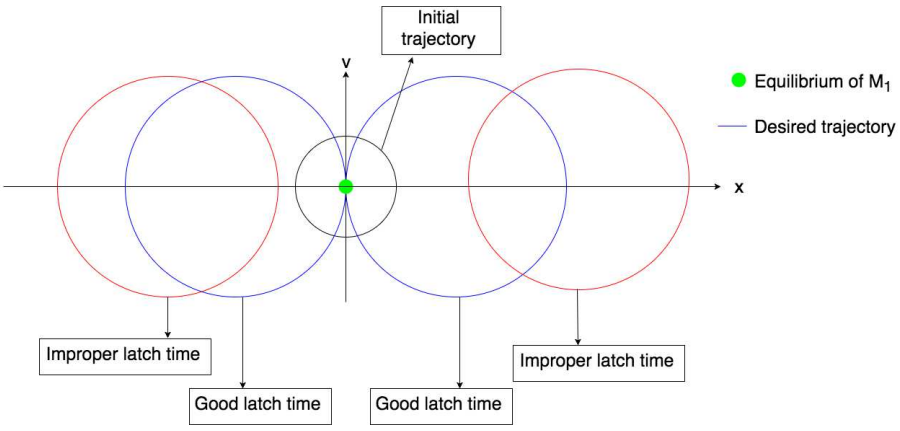

Figure 3.6: Initial trajectories of M_1 and latched trajectories of M_2

In fig.(3.6), we can see that the blue circles pass the equilibrium of subsystem M_1 with zero velocity and zero displacement. To find the turn on condition, we should find a way to make M_1 go onto the trajectories that passes the equilibrium of subsystem M_1.

To acheive this, first we consider the system equilibrium position when the latch is on. That is, M_1 and M_2 are connected by the latch as in fig. (3.7).

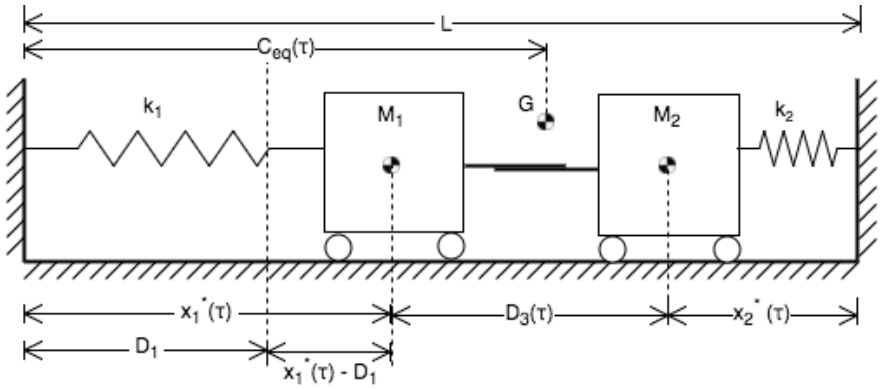

Figure 3.7: New equilibrim postition at the time latch is on

To get the new equilibrium position of overall system, calculate the length of springs k_1 and k_2 by equilibrium of force with a specific length between M_1 and M_2.

$$L = x_1 + x_2 + D_3(\tau), \;\; x_2 = L - x_1 - D_3(\tau)$$

$$\begin{aligned}\sum F_x &= 0 \\ &= K_1(D_1 - x_1) - K_2(D_2 - x_2) \\ &= K_1(D_1 - x_1) - K_2(D_2 - (L - x_1 - D_3(\tau))) \\ &= K_1 D_1 - K_1 x_1 - K_2 D_2 + K_2(L - x_1 - D_3(\tau))\end{aligned}$$

$$\begin{aligned}\Rightarrow -(K_1 + K_2)x_1^* + K_1 D_1 - K_2 D_2 + K_2 L - K_2 D_3(\tau) = 0 \\ \Rightarrow x_1^*(D_3(\tau)) = \frac{K_1 D_1 + K_2(L - D_2 - D_3(\tau))}{K_1 + K_2}\end{aligned} \tag{3.3}$$

Now we have the equilibrium position of the system with a specific $D_3(t_\tau)$. Here x_1^* means the new equilibrium position for M_1.

Note that the new equilibrium is varying with $D_3(t_\tau)$, and the length of it changes with the state which is a time varying value. That is to say, the system will have different equilibrium positions if we turn the latch on at different time.

Next, in order to calculate the potential energy after two subsystem coupled, we need the position of the mass center ($C_{eq}(\tau)$) of the system at time when the latch is on. The symbol x_2^* means the new equilibrium position for M_2

$$\begin{aligned} C_{eq}(D_3(\tau)) &= \frac{M_1 x_1^* + M_2(L - x_2^*)}{M_1 + M_2} \\ &= \frac{M_1 x_1^* + M_2(L - (L - x_1 - D_3(\tau)))}{M_1 + M_2} \\ &= \frac{(M_1 + M_2)x_1^* + D_3(\tau)M_2}{M_1 + M_2} \end{aligned} \tag{3.4}$$

According to our strategy, we need to make M_1 back to its original equilibrium when the distance between this instant position of M_1 and its original position is the longest distance for this coupled system can reach. To achieve these conditions, the system need to have the exact same amount of energy E_{need} after the latch is on. In fig.(3.8), the distance between the position of two M_1 in the upper and bottom subplot indicate the potential energy stored in the spring k_1 and k_2 which the coupled system need to have to make M_1 go back to the equilibrium of subsystem M_1.

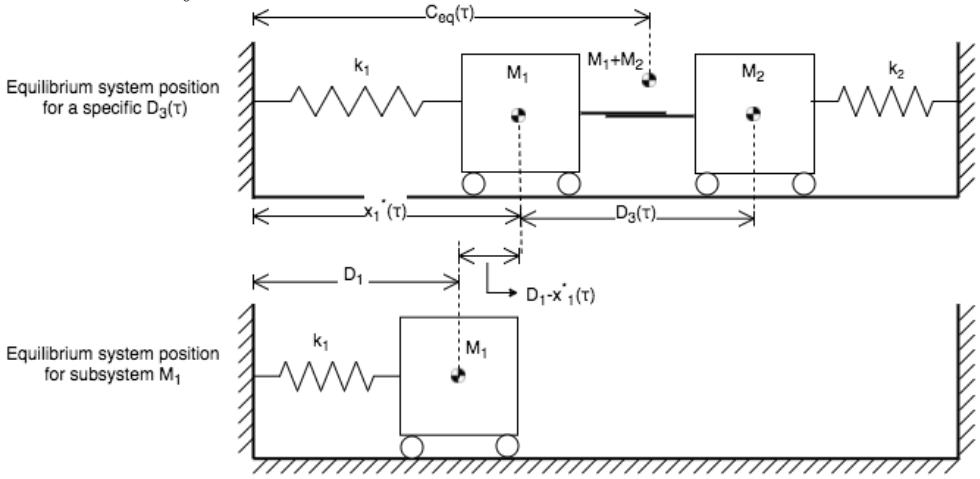

Figure 3.8: System portraits for potential energy

The length for M_1 to go back to its original equilibrium is,

$$D_{need} = x_1^*(t_\tau) - D_1 \tag{3.5}$$

Then we can calculate the exact amount of energy the system need to make M_1 reach the original equilibrium position without passing it.

$$E_{need} = 0.5(K_1 + K_2)D_{need}^2 \tag{3.6}$$

The next things we need to know is when does the system has such conditions. To do this, we need to know the system states at every time step during the process, estimating how much energy will be in the system if we turned on the latch at this instant. If the amount of energy match with E_{need}, we then know that it is the desired time to turn on.

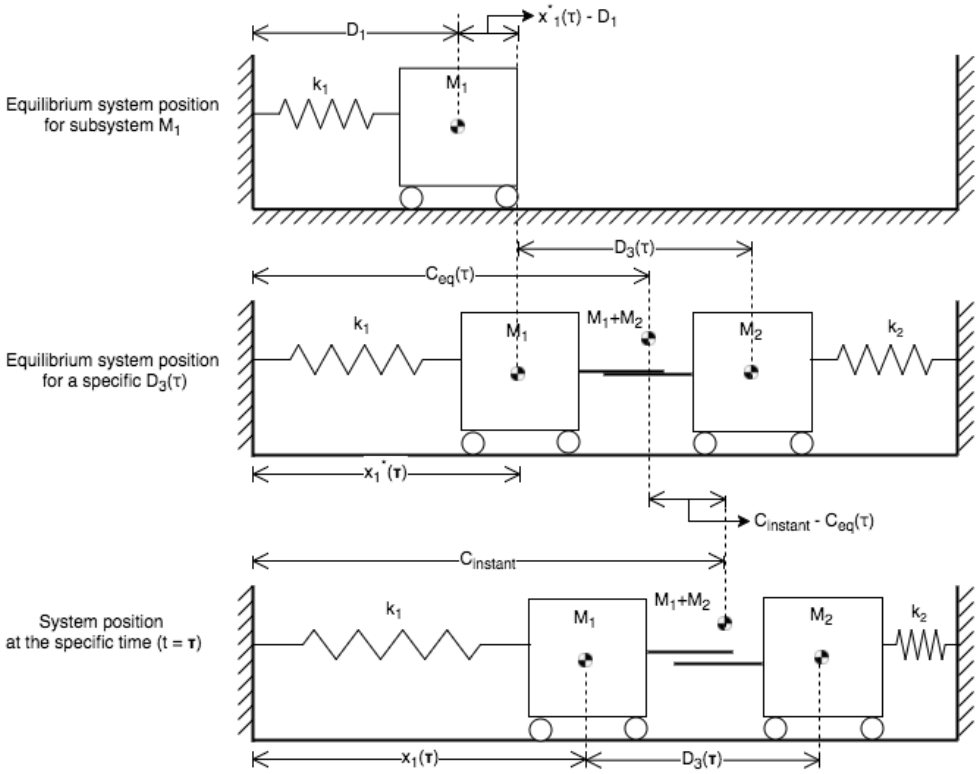

Figure 3.9: Instant systme portrait at the time latch turned on

To explicit illustrate, we draw the instant system scheme along with two different equilibrium system schematic. The first subplot in fig.(3.9) is the equilibrium position for subsystem M_1 and the second suplot is the equilibrium position for coupled M_1 and M_2 system. The third subplot is the system schematic at a specific instant time. Assuming that we have full knowledge of system states, x_1, x_2, v_1, v_2. The position of the mass center $C_{instant}$ at this particular time is,

$$C_{instant} = \frac{M_1 x_1 + M_2(L - x_2)}{M_1 + M_2}$$

Then the potential energy with respect to the coupled system at this instant is,

$$U_{instant}(D_3(\tau)) = 0.5(K_1 + K_2)(C_{eq}(\tau) - C_{instant})^2 \tag{3.7}$$

Here we are going to make a assumption that it is a inelastic collision when the latch between M_1 and M_2 is turned on. From theory of conservation of momentum in eq.(3.2), we have the velocity of the two masses after we turn on the latch,

$$V_{inelastic} = \frac{M_1 v_1 + M_2 v_2}{M_1 + M_2}$$

Then the kinetic energy in the system will be,

$$K_{instant} = 0.5(M_1 + M_2)V_{inelastic}^2 \tag{3.8}$$

By combining the equations (3.6), (3.8), (3.7), we get,

$$\begin{aligned} E_{need}(D_3(\tau)) &= E_{instant} \\ &= K_{instant} + U_{instant}(D_3(\tau)) \end{aligned} \tag{3.9}$$

Finally, solve eq.(3.9) respect to $D_3(\tau)$. We explicitly show the equation in the appendix.

With this $D_3(\tau)$, it means that the distance between M_1 and M_2 needs to equal to $D_3(\tau)$ in order to minimize the vibration of M_1 . Otherwise, the latch should not be turned on at this moment.

Now, the hard part of the problem was solved. We had ensured the subsystem M_1 is able to go back to its equilibrium position with zero velocity. The remain part of algorithm is waiting to reach the original equilibrium of M_1. When this condition is fullfilled, turn off the latch. The condition to turn off the latch is,

$$x_1 = 0,\ v_1 = 0$$

To avoid missing this condition, we can set a tolerance for it.

$$|x_1| < \epsilon_1,\ |v_1| < \epsilon_2$$

where ϵ_1 and ϵ_2 are two small numbers. The reason we do this relaxation is that we can still get a good result without using extremely high frequency to sample system states.

3.3 Simulation results

We show four results under different conditions as follow.

Case 1

$$\begin{cases} x_1(0) = 0.7 \\ x_2(0) = 0 \\ v_1(0) = 0 \\ v_2(0) = 0 \end{cases} \qquad \begin{cases} w_{M1} = 1.0\pi \\ w_{M2} = 1.4\pi \end{cases} \tag{3.10}$$

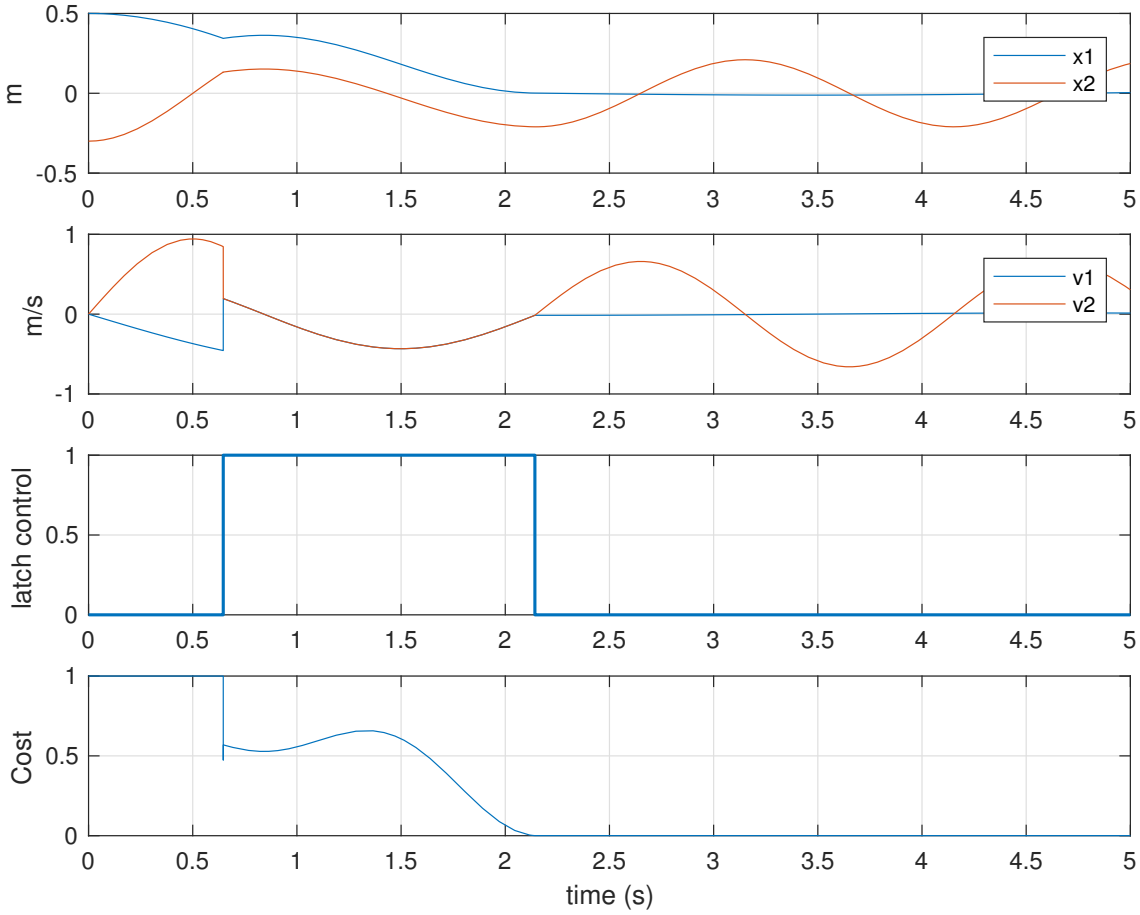

Figure 3.10: Case1 time domain simulation

Case 2

$$\begin{cases} x_1(0) = 0.5 \\ x_2(0) = -0.3 \\ v_1(0) = 0 \\ v_2(0) = 0 \end{cases} \qquad \begin{cases} w_{M1} = 1.0\pi \\ w_{M2} = 1.4\pi \end{cases} \tag{3.11}$$

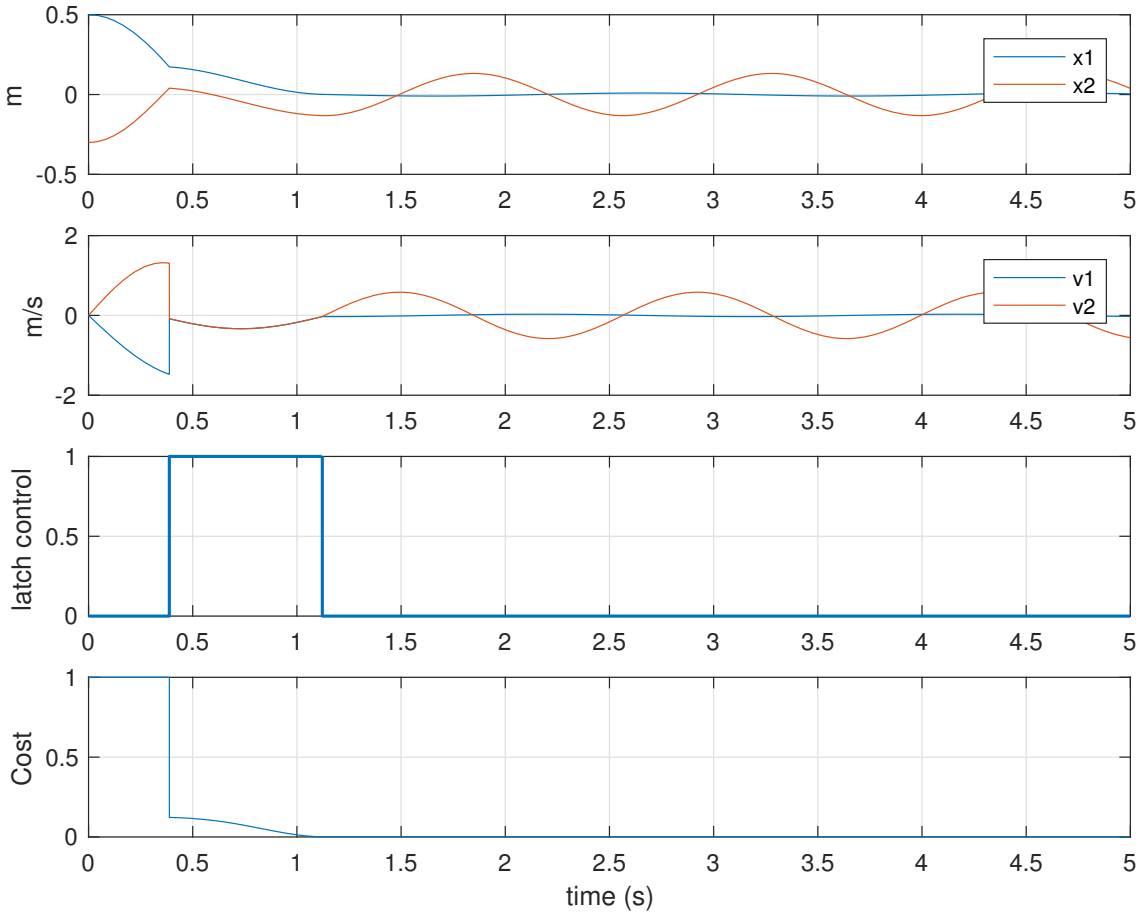

Figure 3.11: Case2 time domain simulation

Case 3

$$\begin{cases} x_1(0) = 0.5 \\ x_2(0) = -0.3 \\ v_1(0) = 0 \\ v_2(0) = 0 \end{cases} \qquad \begin{cases} w_{M1} = 1.0\pi \\ w_{M2} = 1.0\pi \end{cases} \tag{3.12}$$

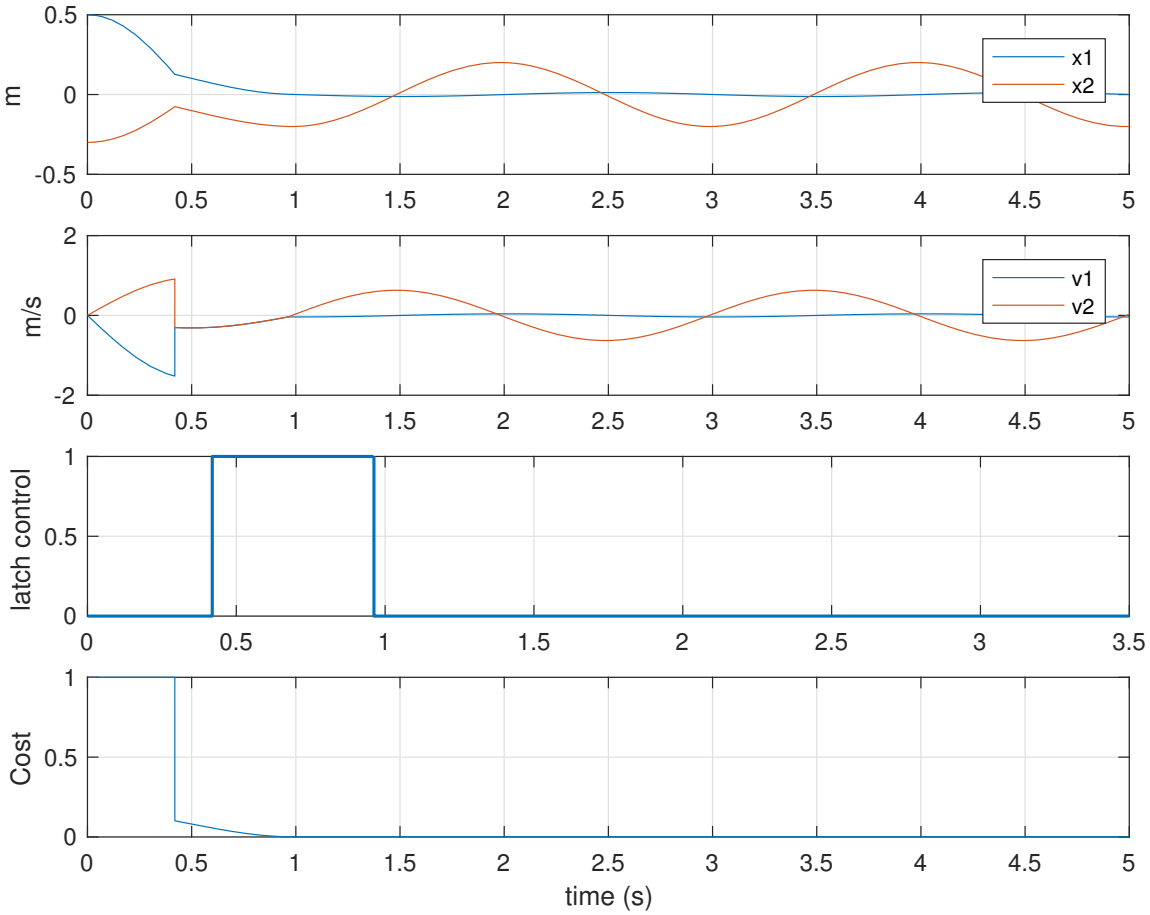

Figure 3.12: Case3 time domain simulation

Case 4

$$\begin{cases} x_1(0) = 0.5 \\ x_2(0) = -0.3 \\ v_1(0) = 0 \\ v_2(0) = 0 \end{cases} \qquad \begin{cases} w_{M1} = 0.4\pi \\ w_{M2} = 1.0\pi \end{cases} \tag{3.13}$$

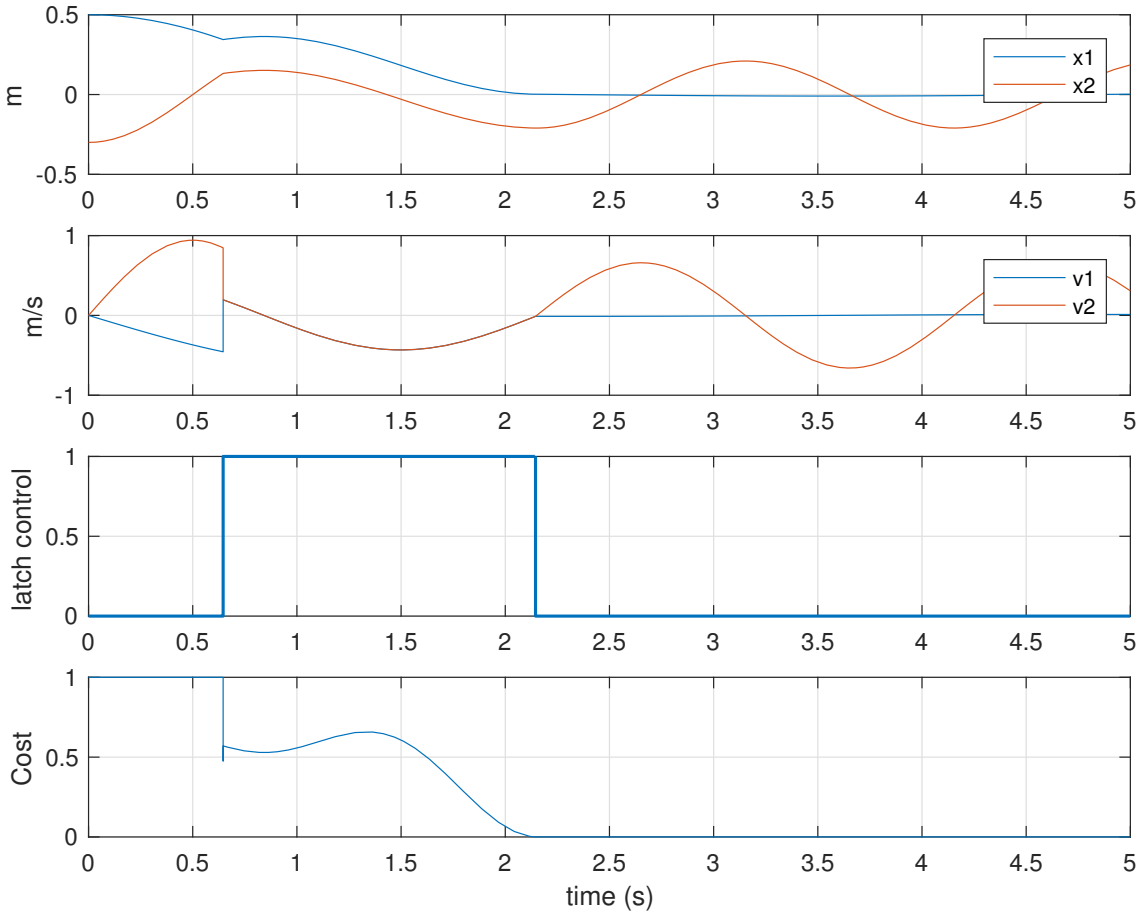

Figure 3.13: Case4 time domain simulation

Chapter 4

Existence and Uniqueness for nonideal implement

In the last chapter, we showed that there is an analytic solution under ideal conditions. However, in reality the ideal conditions will never be achieved. There always exists some time delay before the latch is fully on. Furthermore, in real-time application, there always exist external froces from the enviornment. In this chapter we use an exhaustive method to get the final cost by sweeping through every possible time for the latch to turn on and turn off. We define our normalized cost function the same as eq.(3.1).

$$\begin{aligned} J &= \frac{Final\ Enery\ in\ M_1}{Initial\ Energy\ in\ M_1} \\ &= \frac{(M_1 v_1^2 + K_1 x_1^2)}{(M_1 v_{10}^2 + K_1 x_{10}^2)} \end{aligned}$$

As for the nonideal latch element, we choose maximum damping coefficient and the time constant for a latch to be,

$$\begin{cases} B_{Max} = 500 \quad (N - m/s) \\ \tau = 10^{-3} \quad (s) \end{cases}$$

4.1 Describe the optimization procedure

First, we choose a set of system parameters, initial condition and descriptions of excitation using this specific system to run hundreds of simulation with different single switch control event. Each of the simulation has a different process of control event which means that they have different turn on and turn off time. The time t_{on} in fig.(2.2) corresponds to the x position and the time t_{off} corresponds to the y position and the final cost for the system

with this set of control event, t_{on} and t_{off}, corresponds to the z postition in the explicit cost plot fig.(4.1).

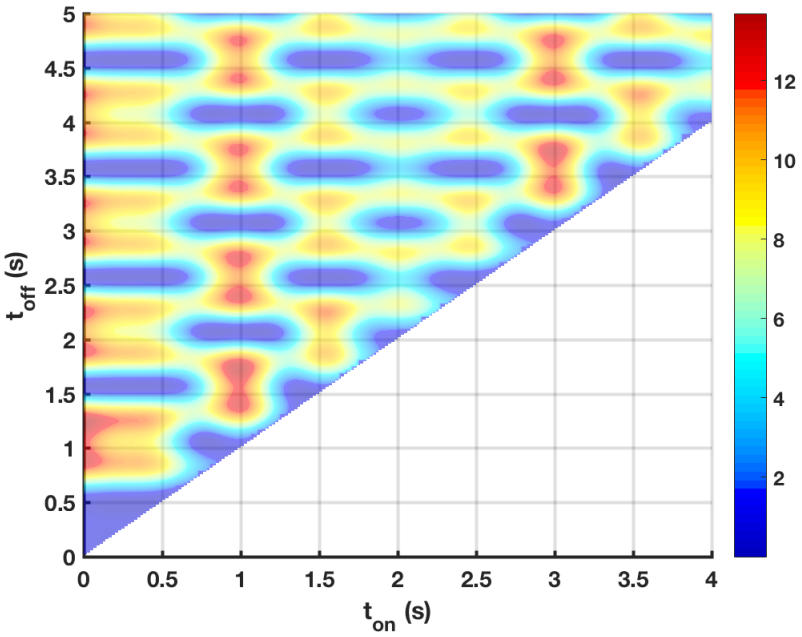

Figure 4.1: Cost plot

The whole figure generating process is shown in fig.(4.2). We restrict the latch need to be in off-state at the begining. In consequence, our turn-on time will always happen earlier than turn-off time. Thus, the cost plot appears above the line $t_{on} = t_{off}$, since $t_{off} > t_{on}$ does not exist.

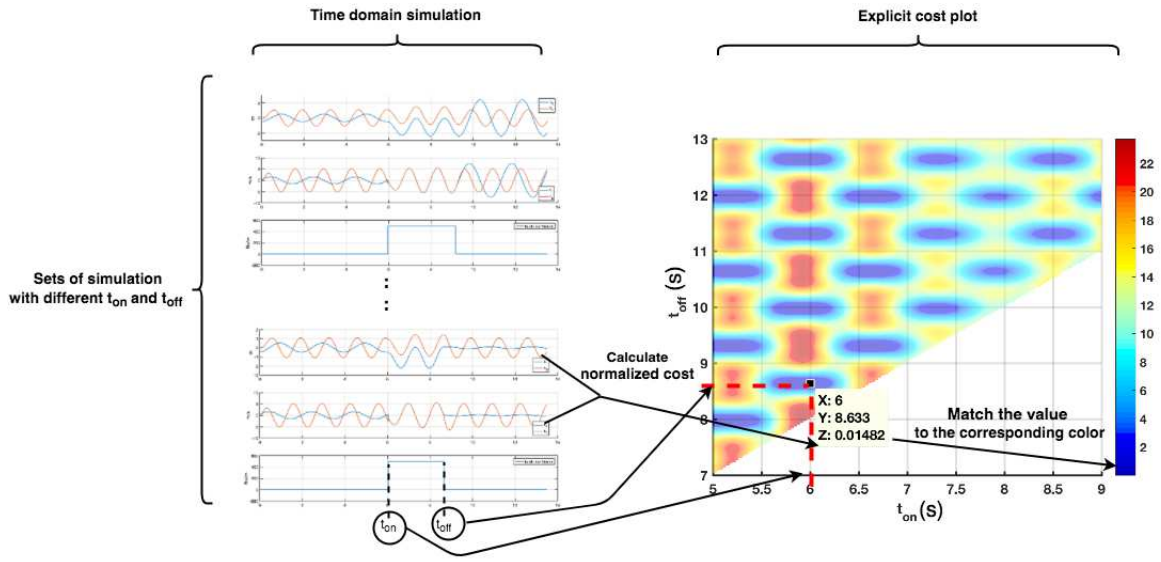

Figure 4.2: Procedure of creating cost plot

Since subsystem M_1 and M_2 are two second order periodic systems, the cost value repeats itself in the direction of x-axis according to the period of subsystems M_1 and M_2. As you can see in fig.(4.3) that the pattern repeats itself. Thus, we know that by choosing finite numbers of t_{on}, it is possible to show all distinct cost caused by different t_{on}. To get the unrepeating part of the cost, we need to know the approximate common multiple period of subsystem M_1 and M_2. Or, for excited system, the vibration frequency of M_2 is determind by the excitation force. As a result, we should consider the period of M_1 and external force instead.

System without excitation

$$T_{M1} = \frac{w_{M1}}{2\pi}$$
$$T_{M2} = \frac{w_{M2}}{2\pi}$$
$$T_{common} = lcm(T_{M1}, T_{M2}) \tag{4.1}$$

System with excitation

$$T_{M1} = \frac{w_{M1}}{2\pi}$$
$$T_{M2} = \frac{w_f}{2\pi}$$
$$T_{common} = lcm(T_{M1}, T_{M2}) \tag{4.2}$$

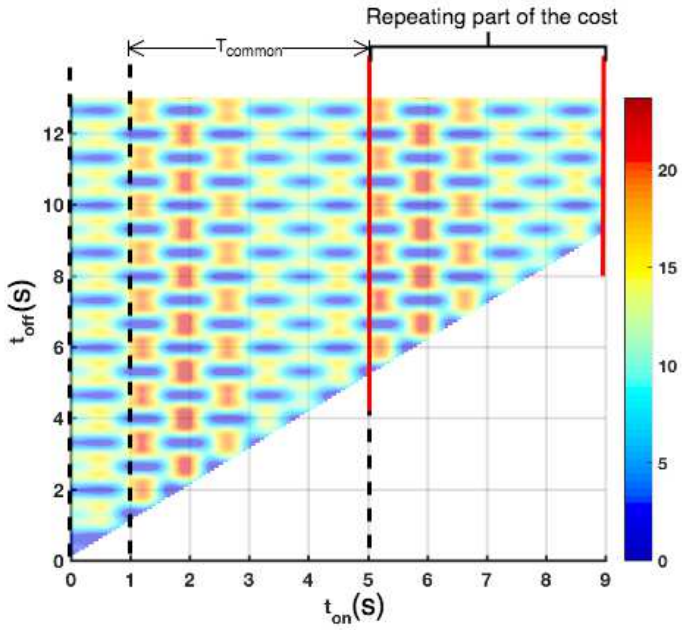

Figure 4.3: Procedure of getting repeating pattern from cost plot

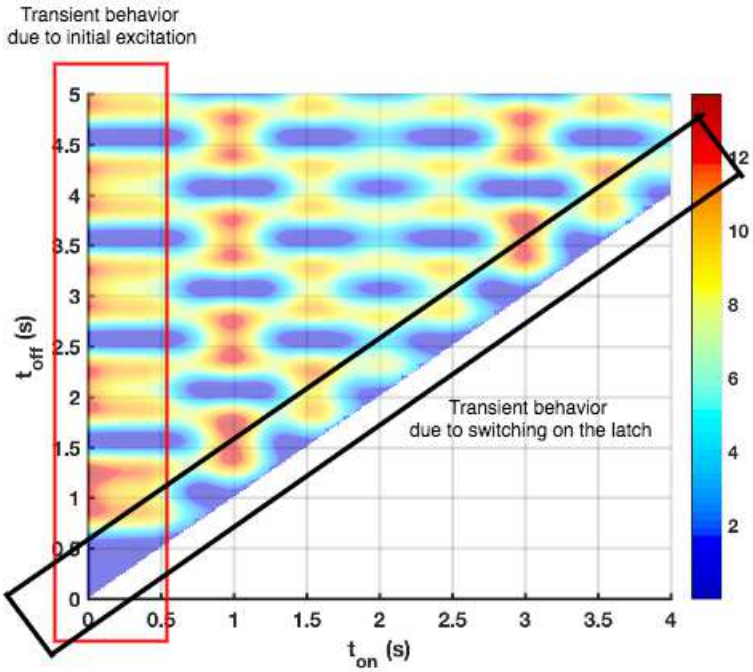

Figure 4.4: Transients in the cost plot

To aviod transient behavior to show up in the cost plot like in fig.(4.4), and affect optimization procedure, we exclude some of the combinations of t_{on} and t_{off}. As a result, the

x-axis (representing t_{on}) of the cost plot begins at a nonzero value, and so does the y-axis (representing t_{off}) starts after t_{on} for τ_{s2} of time.

To decide how long should we wait for transient to die out, we examine the dynamic equation,

$$\begin{aligned} m\ddot{x}(t) + b\dot{x}(t) + kx(t) &= F(t) \\ \Rightarrow \ddot{x}(t) + \frac{b}{m}\dot{x}(t) + \frac{k}{m}x(t) &= \frac{F(t)}{m} \end{aligned} \tag{4.3}$$

Let,

$$\begin{aligned} w_n &= \sqrt{\frac{k}{m}} \\ \zeta &= \frac{b}{C_c} \\ C_c &= 2\sqrt{km} \end{aligned}$$

Equation 4.3 becomes,

$$\Rightarrow \ddot{x}(t) + 2\zeta w_n \dot{x}(t) + w_n^2 x(t) = \frac{F(t)}{m} \tag{4.4}$$

The solution for equation 4.4 is,

$$\begin{aligned} x(t) &= c_1 e^{(-\zeta w_n + i w_n \sqrt{1-\zeta^2})t} + c_2 e^{(-\zeta w_n - i w_n \sqrt{1-\zeta^2})t} \\ &= e^{-\zeta w_n t}\left\{c_1\left(e^{it\sqrt{1-\zeta^2}} + c_2 e^{-it\sqrt{1-\zeta^2}}\right)\right\} \end{aligned}$$

From Euler equation $e^{ix} = \cos x + i \sin x$,

$$\begin{aligned} &= e^{-\zeta w_n t}\left\{c_1\left(\cos\sqrt{1-\zeta^2}t + i\sin\sqrt{1-\zeta^2}t\right) + c_2\left(\cos\sqrt{1-\zeta^2}t - i\sin\sqrt{1-\zeta^2}t\right)\right\} \\ &= e^{-\zeta w_n t}\left\{(c_1+c_2)\cos\sqrt{1-\zeta^2}t + (c_1-c_2)\,i\sin\sqrt{1-\zeta^2}t\right\} \end{aligned} \tag{4.5}$$

Since $c_1 - c_2$ is always pure imaginary or zero for problem with actual physical meaning, equation 4.5 can be written as,

$$x(t) = e^{-\zeta w_n t}\left\{A\cos\sqrt{1-\zeta^2}t + B\sin\sqrt{1-\zeta^2}t\right\} \tag{4.6}$$

Where A and B are constants.
The exponential term $e^{-\zeta w_n t}$ in equation (4.6) indicate that the solution is exponentially decaying with time. The typical definition of settling time (τ_s) is $\pm$ 1% of the its final value.

$$\begin{aligned} e^{-\zeta w_n t} &= 0.01 \\ -\zeta w_n t &= \ln 0.01 \\ t = \tau_s &= -\frac{\ln 0.01}{\zeta w_n} \end{aligned} \tag{4.7}$$

For τ_{s1}, since there is no damper within subsystem M_1, subsystem M_2 is the only part of the system that will have transient behavior. By considering w_{M2} and its dampeing coefficients ζ, the settling time τ_{s1} can be decided.

$$\tau_{s1} = \frac{\ln 0.01}{\zeta_{M2}} \sqrt{\frac{M_2}{K_2}} \tag{4.8}$$

Another transient behavior happened when the latch is being switch on. Unlike the last transient we only include subsystem M_2 into consideration, we need to calculate the settling time for the overall system τ_{s2}, because two subsystems are already connected by the latch element becoming one coupling system. That is, we need to consider the overall damping ratio ζ_{all} and the overall natural frequency w_{all}.

First, calculating $\zeta_{all} \Rightarrow$

$$\begin{aligned}
\zeta_{M2} &= \frac{b_2}{2\sqrt{K_2 M_2}} \\
\Rightarrow b_2 &= 2\zeta_{M2}\sqrt{K_2 M_2} \\
\zeta_{all} &= \frac{b_2}{2\sqrt{(K_1+K_2)(M_1+M_2)}} \\
&= \frac{\zeta_{M2}\sqrt{K_2 M_2}}{(K_1+K_2)(M_1+M_2)}
\end{aligned}$$

w_{all} can derived from equaitons $\Rightarrow$

$$\begin{aligned}
w_{M2} &= \sqrt{\frac{K_2}{M_2}} \\
w_{all} &= \sqrt{\frac{K_1+K_2}{M_1+M_2}}
\end{aligned}$$

Then know the relative settling time we need for the overall system,

$$\begin{aligned}
\tau_{s2} &= -\frac{\ln 0.01}{\zeta_{all} w_{all}} \\
&= \frac{(M_1+M_2)\ln 0.01}{\zeta_{M2}\sqrt{K_2 M_2}}
\end{aligned}$$

In our system model we assumed that $M_1 = M_2$,

$$\begin{aligned}\tau_{s2} &= \frac{(M_1+M_2)\ln 0.01}{\zeta_{M2}\sqrt{K_2 M_2}} \\ &= \frac{\ln 0.01}{\zeta_{M2}}\sqrt{\frac{(M_1+M_2)^2}{K_2 M_2}} \\ &= \frac{\ln 0.01}{\zeta_{M2}}\sqrt{\frac{4M_2^2}{K_2 M_2}} \\ &= \frac{2\ln 0.01}{\zeta_{M2}}\sqrt{\frac{M_2}{K_2}} = 2\tau_{s1}\end{aligned}$$

Thus we can conclude that the settling time for coupled system (τ_{s2}) needs to be two times greater than τ_{s1}.

If chose $\zeta_{M2} = 0.707$ and $w_{M2} = \pi$, the settling time τ_{s1} for the system is 2.07 seconds. From equation(4.7), we know the settling time of the system is negative correlated to the natural frequency. Since we are not going to examine w_{M_2} smaller than π and we only use $\zeta_{M2} = 0.707$, we choose $\tau_{s1} = \tau_{s2} = 5$ seconds to make all transient behavior smaller than one percent of their initial value.

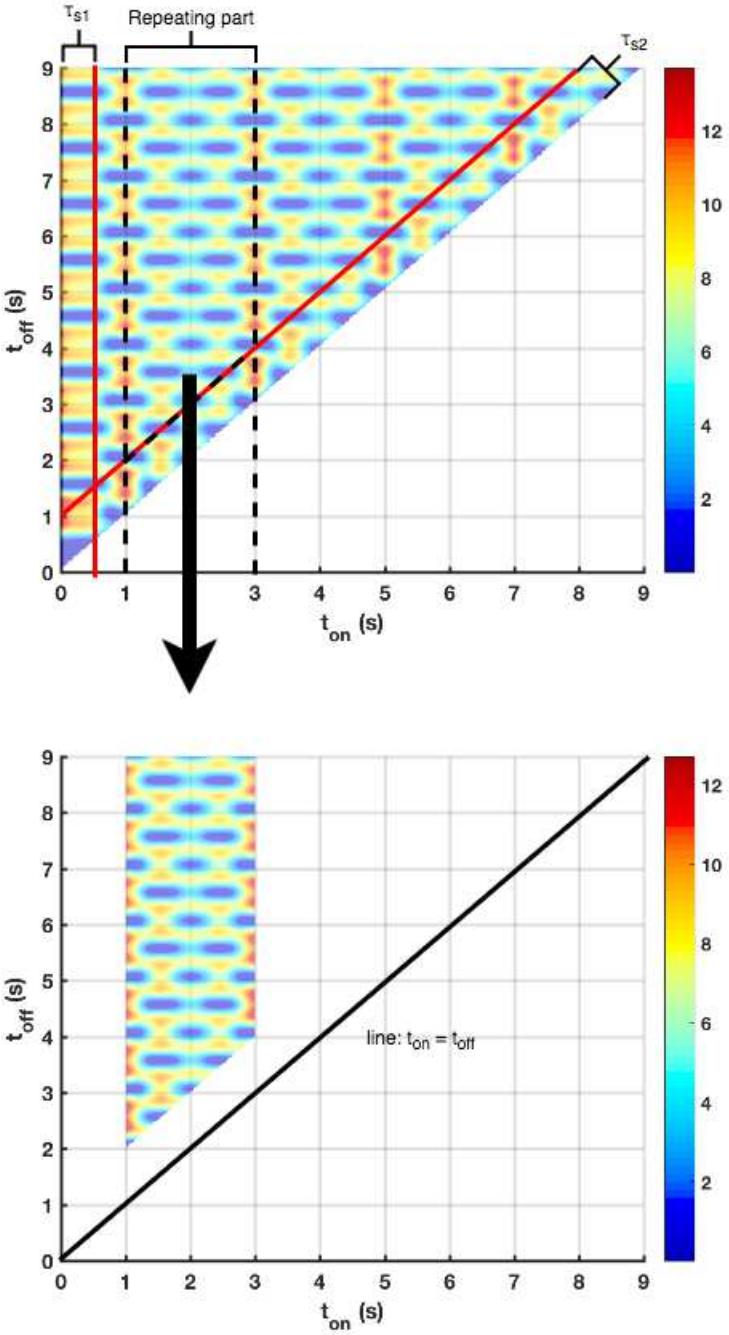

Figure 4.5: The essential part for all possible combinations of t_{on} and t_{off}

4.2 Plots and results

In this section, we choose a period of 5 seconds to get rid of the transient. The color bar in fig.(4.6, 4.7) indicates as the cost value of the system after finished the control process. If the value of the cost is smaller than one, it means that the control event is effective to reduce the energy in M_1. On the contrary, if the value is greater than one, it's not the desired set of t_{on} and t_{off} for the control event.

System without excitation

$$\begin{cases} x_1(0) = -0.5 \\ x_2(0) = 0 \\ v_1(0) = 0.3 \\ v_2(0) = 0 \end{cases} \qquad \begin{cases} w_{M1} = \pi \\ w_{M2} = 2\pi \end{cases} \tag{4.9}$$

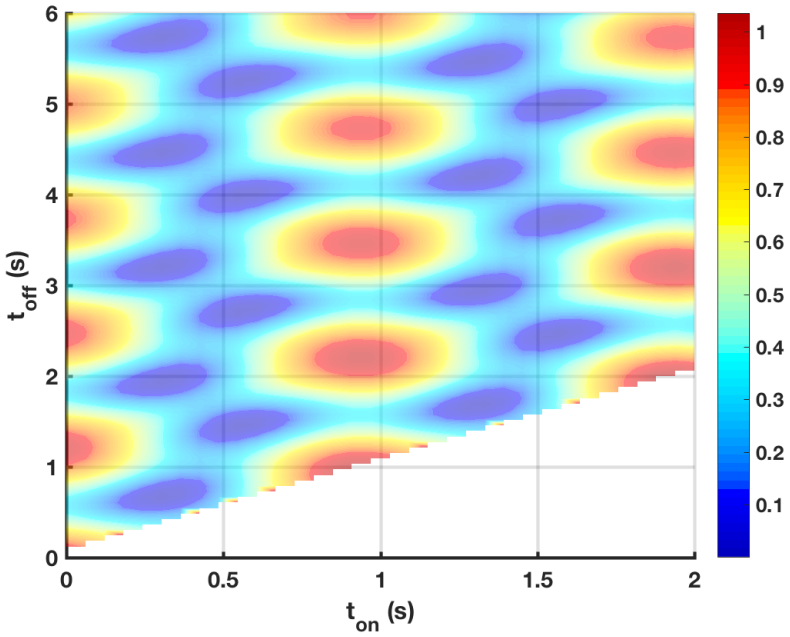

Figure 4.6: Cost plot for system without excitation

System with excitation

$$\begin{cases} x_1(0) = -0.5 \\ x_2(0) = 0 \\ v_1(0) = 0.3 \\ v_2(0) = 0 \end{cases} \qquad \begin{cases} w_{M1} = \pi \\ w_{M2} = 2\pi \\ w_f = 0.8\pi \\ \phi = 0 \end{cases} \tag{4.10}$$

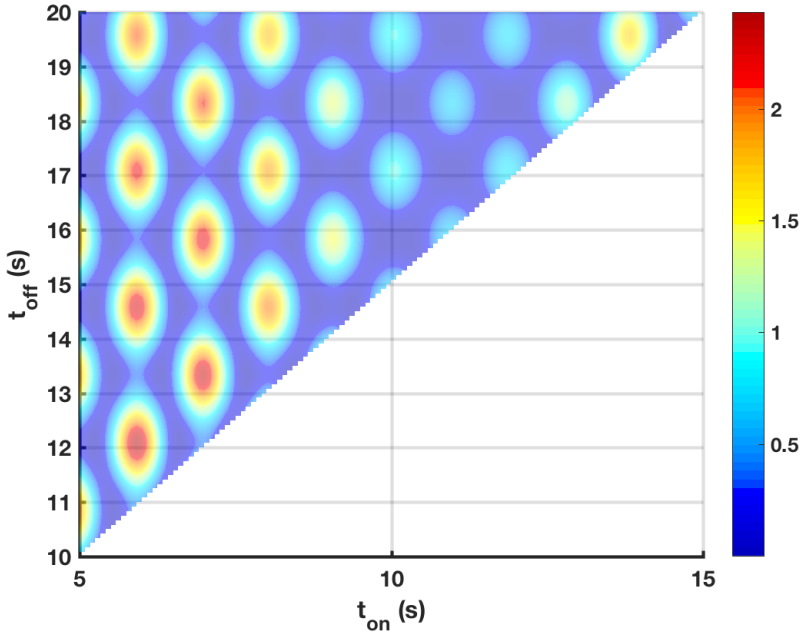

Figure 4.7: Cost plot for system with excitation

In fig.(4.6),(4.7), the cost that is smaller than the value of one exists in both figures. That is to say, no matter the system is under excitation or not, it is possible to find a set of t_{on} and t_{off} to make the energy in M_1 less than its initial value.

Chapter 5

Switch time condition

In chapter 3, we have already derived a control method to minimized the vibration of M_1 under ideal conditions. However, if the system did not have the ideal properties which the control algorithm needs, such as absence of external excitation and ideal latch behavior, then the method is not applicable. Nevertheless, if the objective is to make M_1 possess as less energy as possible, it still only can be achieved when the velocity and the distance between neutral position of M_1 are both at its possible minimum. Thus, the switch-off condition (C_{off}) in fig.(3.2) is still valid regardless to have idea conditions or not. The switch-on condition (C_{on}) is the only unknown condition to us for now. To find C_{on} for nonideal situations, we focus on the minimum in the cost plots such as fig.(4.7) and investigate the system states and find out what is the common attribute of the states that make a proper latch-on decistion causing low final cost.

5.1 Describe the procedure

To find out what is the condition (C_{on}) for latch being turned on, we need to know where the minimum of the final cost occurs. The minimum cost at each t_{on} can be found by extracting the data from our explicit cost plot fig.(4.7). With this t_{on}, the next step is to track back to the time domain simulation to get the system state at t_{on}. By plotting and connecting the states of M_1 and M_2 on the phase portrait, coloring them according to the corresponding cost value, we create the 3-D figure to illustrate the relationship between states and its possible minimum cost. This procedure is demonstrated in fig.(5.1).

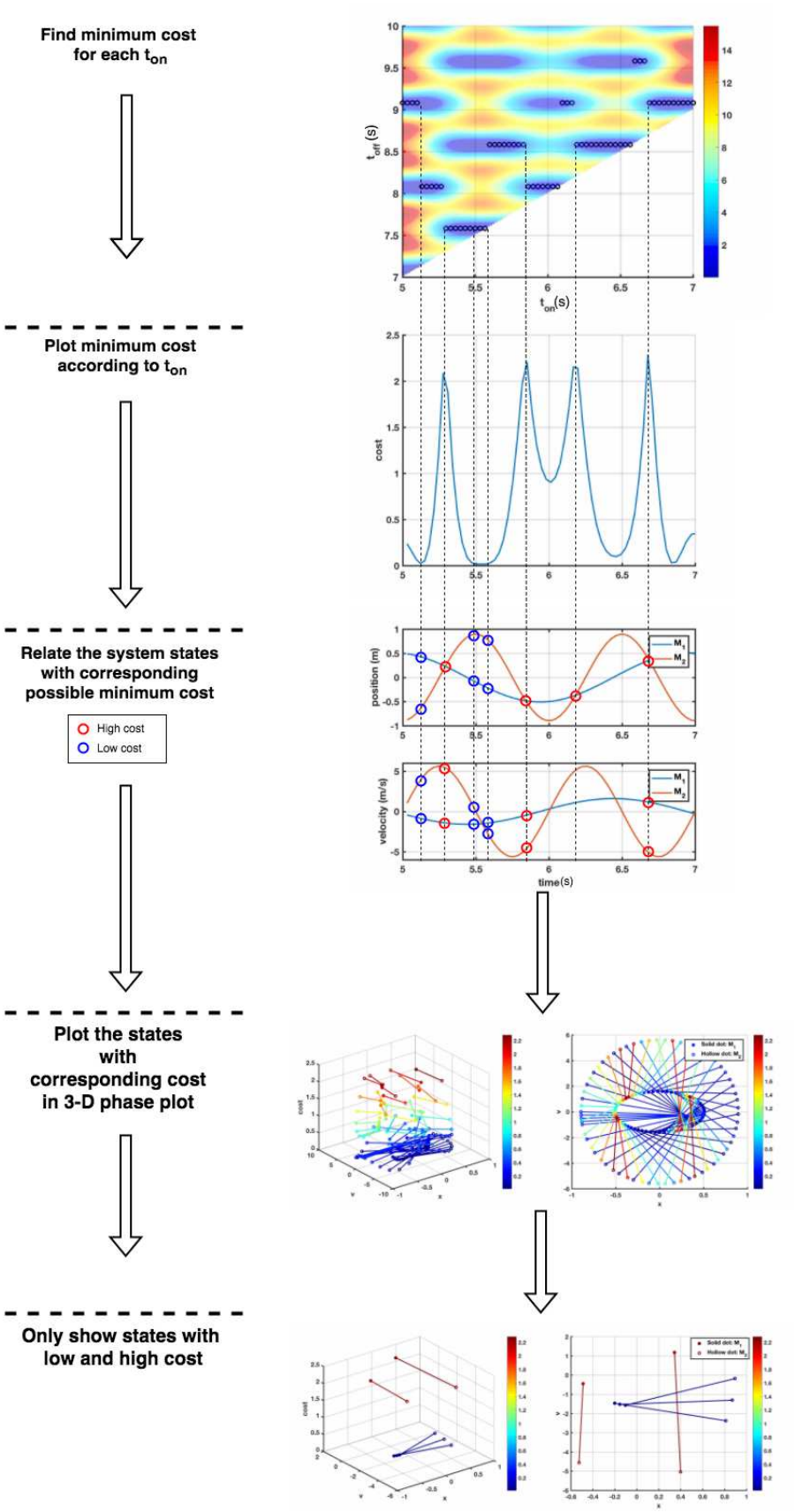

Figure 5.1: Flow chart of the procedure

To understand what role of relative phase angle plays in the control law, we choose the parameters in the steady-state solution that affect the relative phase angle between two masses.

$$\begin{aligned} x_{1ss}(t) &= \mathbb{X}_1 \sin(w_1 t + \phi_1) \\ x_{2ss}(t) &= \mathbb{X}_2 \sin(w_f t + \phi_2) \end{aligned} \tag{5.1}$$

In (5.1), w_1, w_f, ϕ_1, ϕ_2 are the parameters that will change the relative phase. In order to assess the relationship between them, we choose w_1 and ϕ_1 to be the control variables, and only alter the values of w_f or ϕ_2. We will discuss the two different cases of changing w_f and ϕ_2 separately.

5.2 Case study 1 - forcing frequency sweep

To study the effect due to different frequency of external force ($w_f = 3.5\pi,\ 2.6\pi,\ 1.5\pi,\ 0.5\pi$), we use the same system parameters and initial conditions to compare four cases.

$$\text{Initial condition} = \begin{cases} x_1(0) = -0.5 \\ x_2(0) = 0 \\ v_1(0) = 0.3 \\ v_2(0) = 0 \end{cases}, \qquad \begin{cases} w_{M1} = 1.0\pi \\ w_{M2} = 2.0\pi \end{cases} \tag{5.2}$$

case 1-1: $w_f = 3.5\pi$

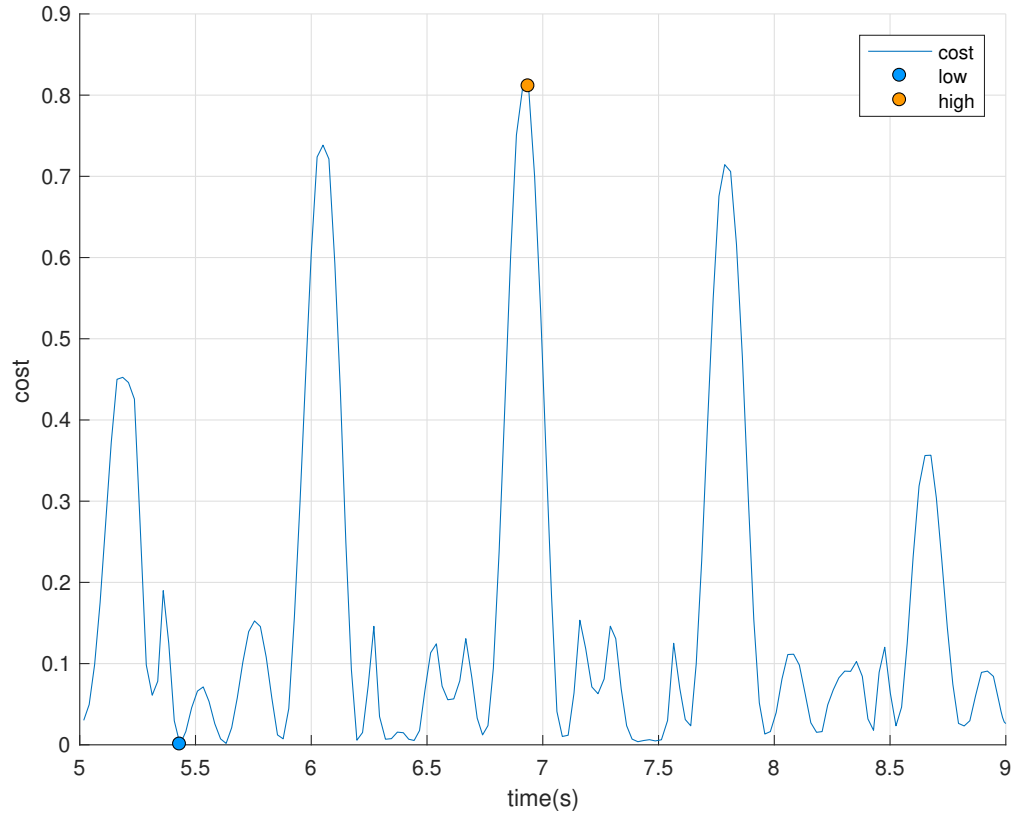

Figure 5.2: Minimum possible cost for every system state

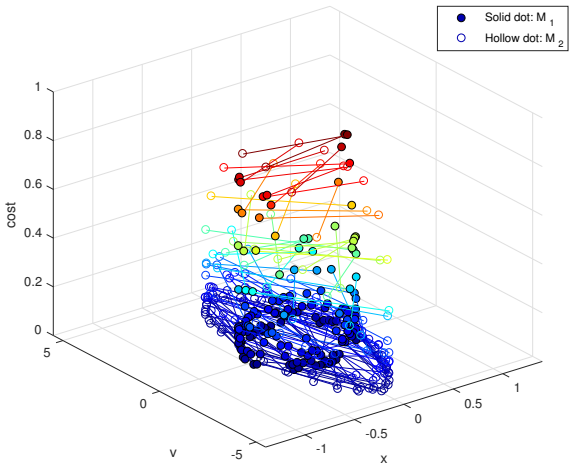

Figure 5.3: 3-D Phase-cost plot

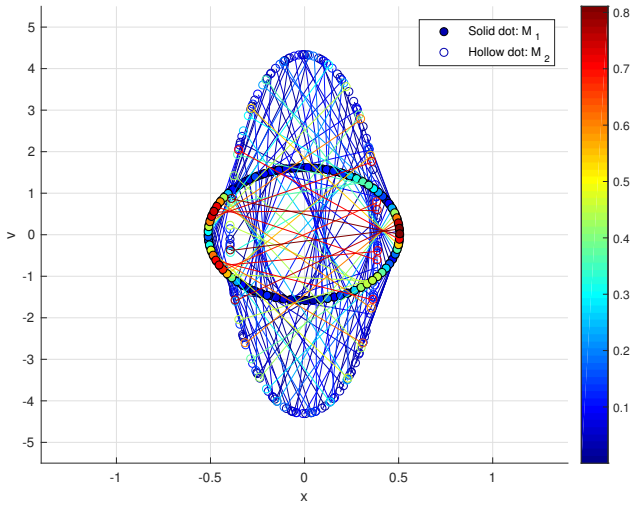

Figure 5.4: 3-D Phase-cost plot - top view

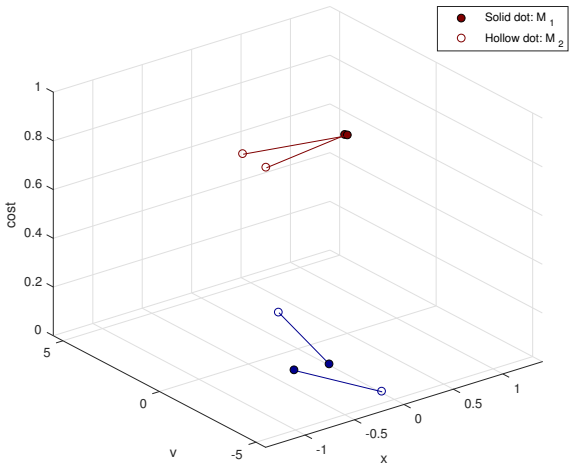

Figure 5.5: Extreme phase cases

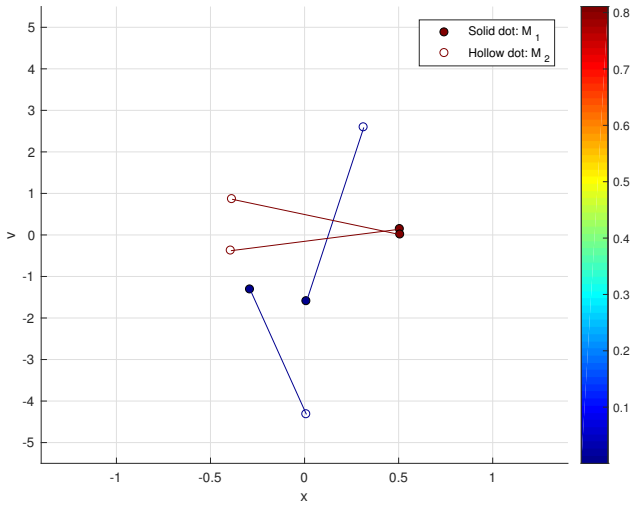

Figure 5.6: Extreme phase cases - top view

case 1-2: $w_f = 2.6\pi$

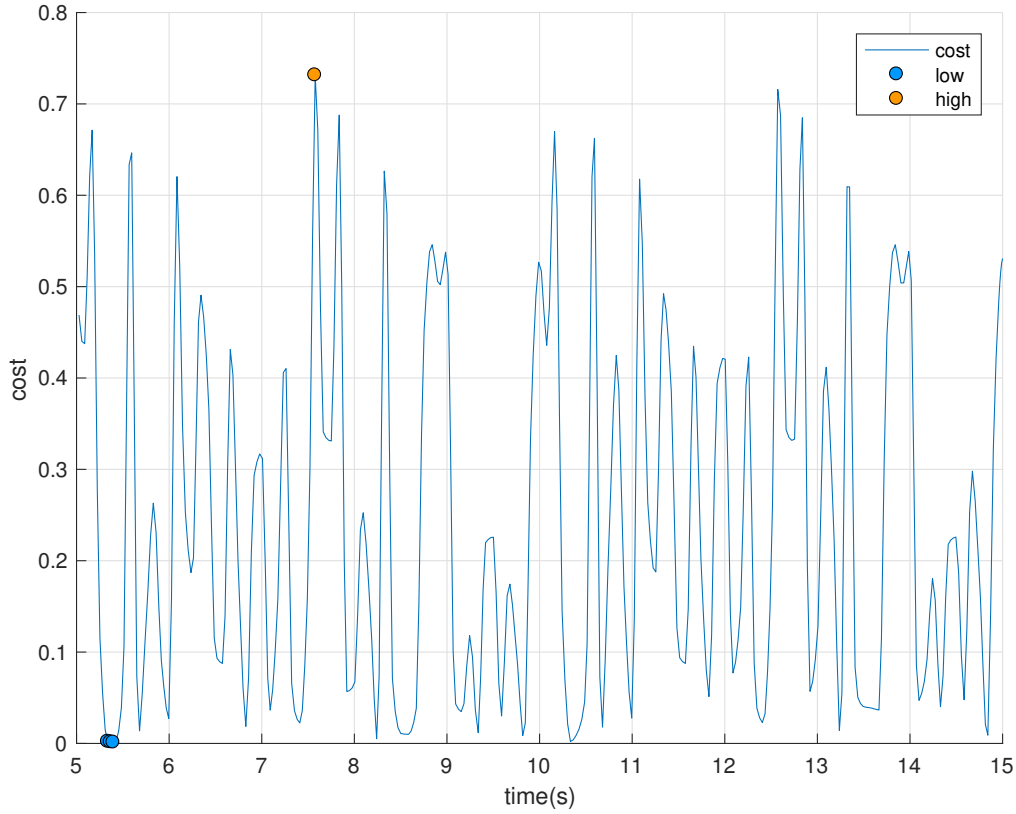

Figure 5.7: Minimum possible cost for every system state

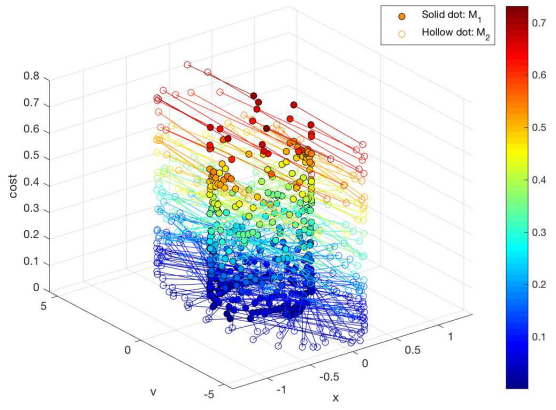

Figure 5.8: 3-D Phase-cost plot

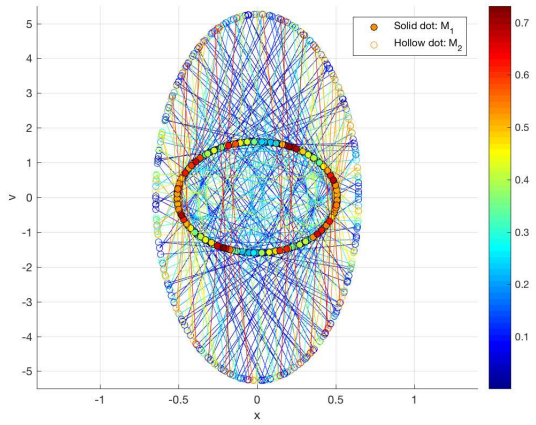

Figure 5.9: 3-D Phase-cost plot- top view

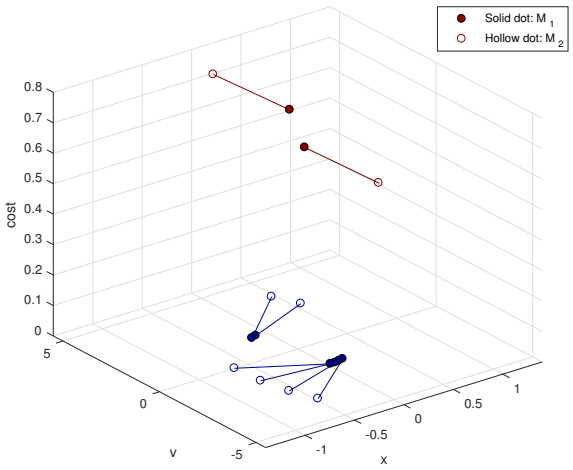

Figure 5.10: Extreme phase cases

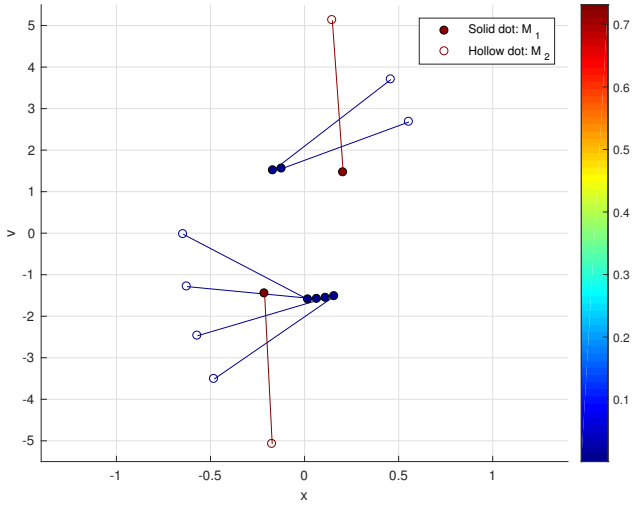

Figure 5.11: Extreme phase cases - top view

case 1-3: $w_f = 1.5\pi$

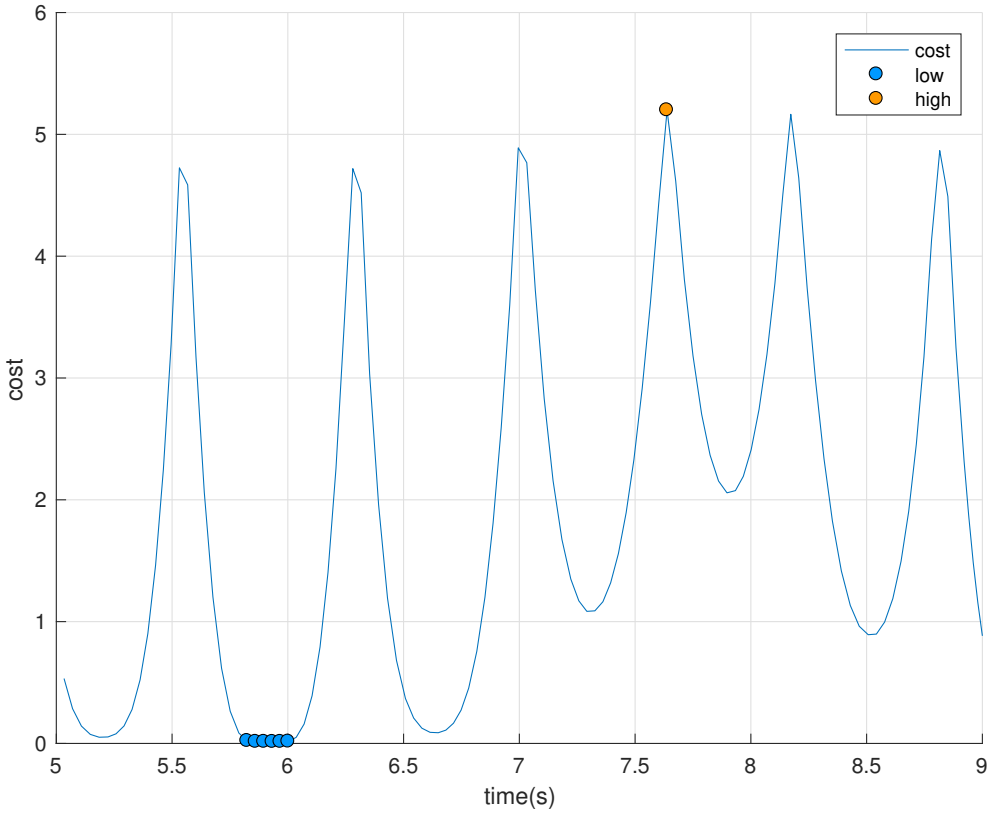

Figure 5.12: Minimum possible cost for every system state

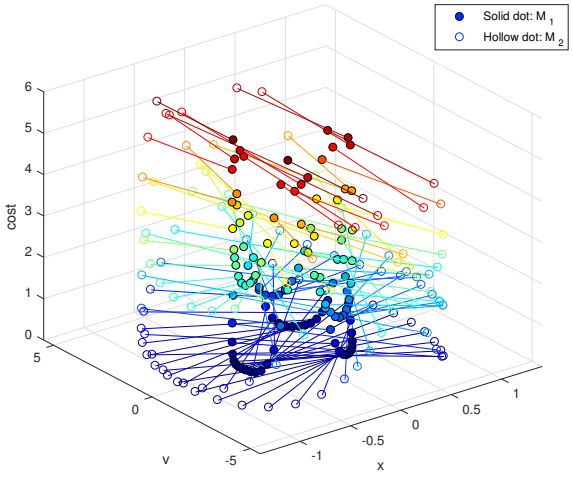

Figure 5.13: 3-D Phase-cost plot

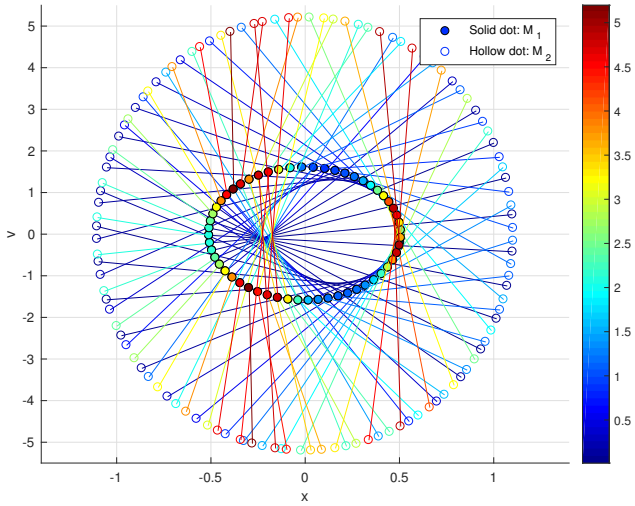

Figure 5.14: 3-D Phase-cost plot - top plan

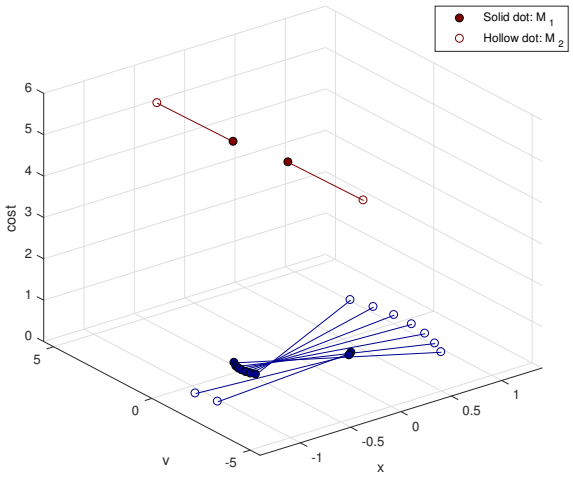

Figure 5.15: Extreme phase cases

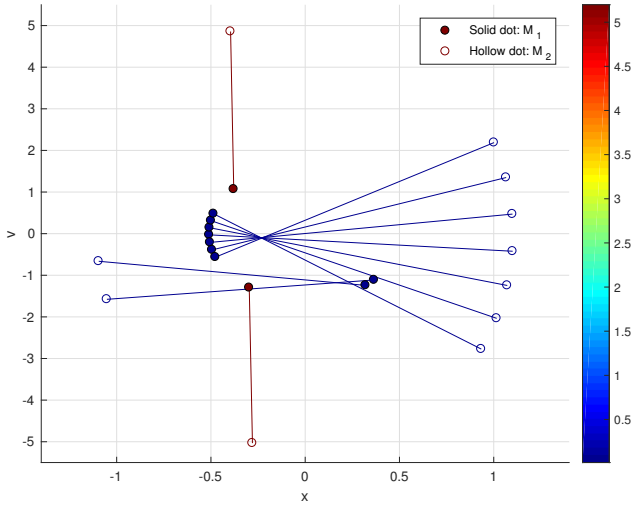

Figure 5.16: Extreme phase cases - top view

case 1-4: $w_f = 0.5\pi$

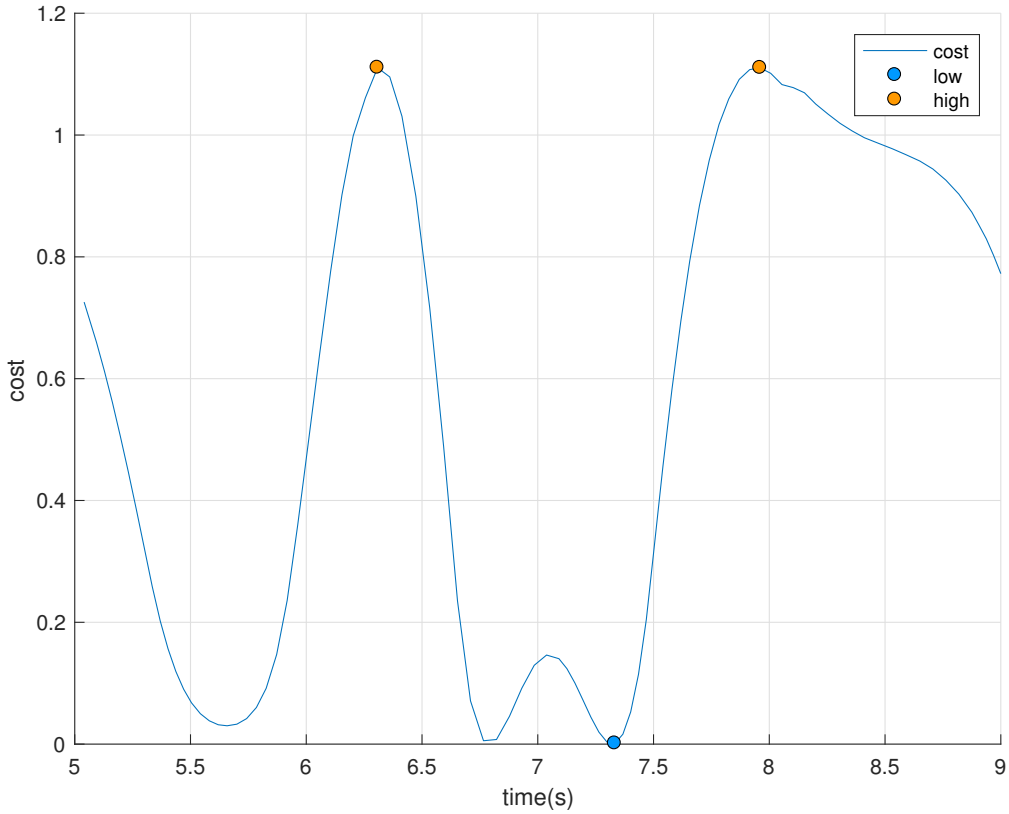

Figure 5.17: Minimum possible cost for every system state

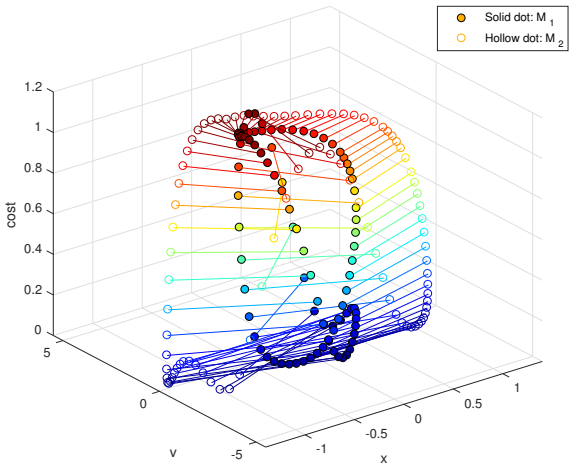

Figure 5.18: 3-D Phase-cost plot

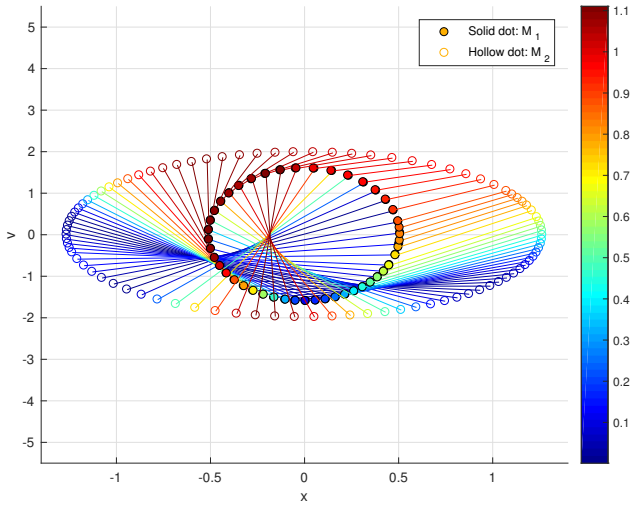

Figure 5.19: 3-D Phase-cost plot - top plan

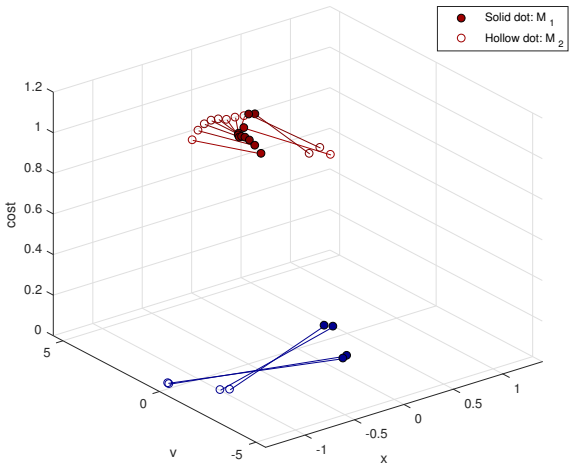

Figure 5.20: Extreme phase cases

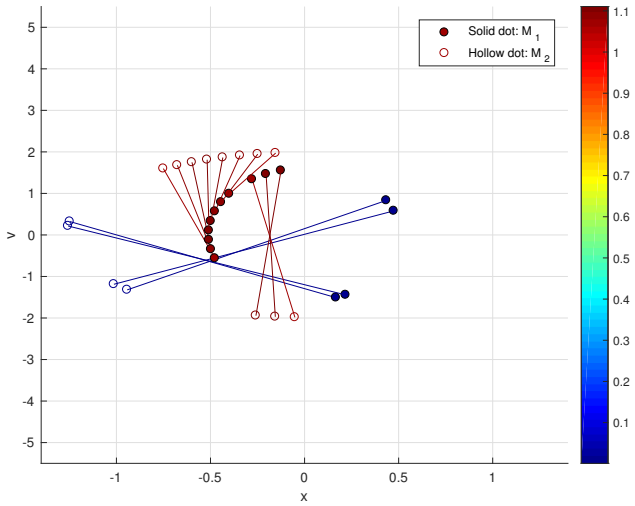

Figure 5.21: Extreme phase cases - top view

5.3 Case study 2 - forcing phase sweep

To study the effect due to different phase angle of external force ($\phi = 0,\ \pi/4,\ \pi/2,\ 3\pi/4,\ \pi$), we use the same system parameters and initial conditions to compare five cases.

$$\text{Initial condition} = \begin{cases} x_1(0) = -0.5 \\ x_2(0) = 0 \\ v_1(0) = 0.3 \\ v_2(0) = 0 \end{cases}, \quad \begin{cases} w_{M1} = 1.0\pi \\ w_{M2} = 2.0\pi \end{cases} \tag{5.3}$$

$$\text{External Force} = \begin{cases} w_f = 1.5\pi \\ F_A = 50 \end{cases} \tag{5.4}$$

case 2-1: $\phi = 0$

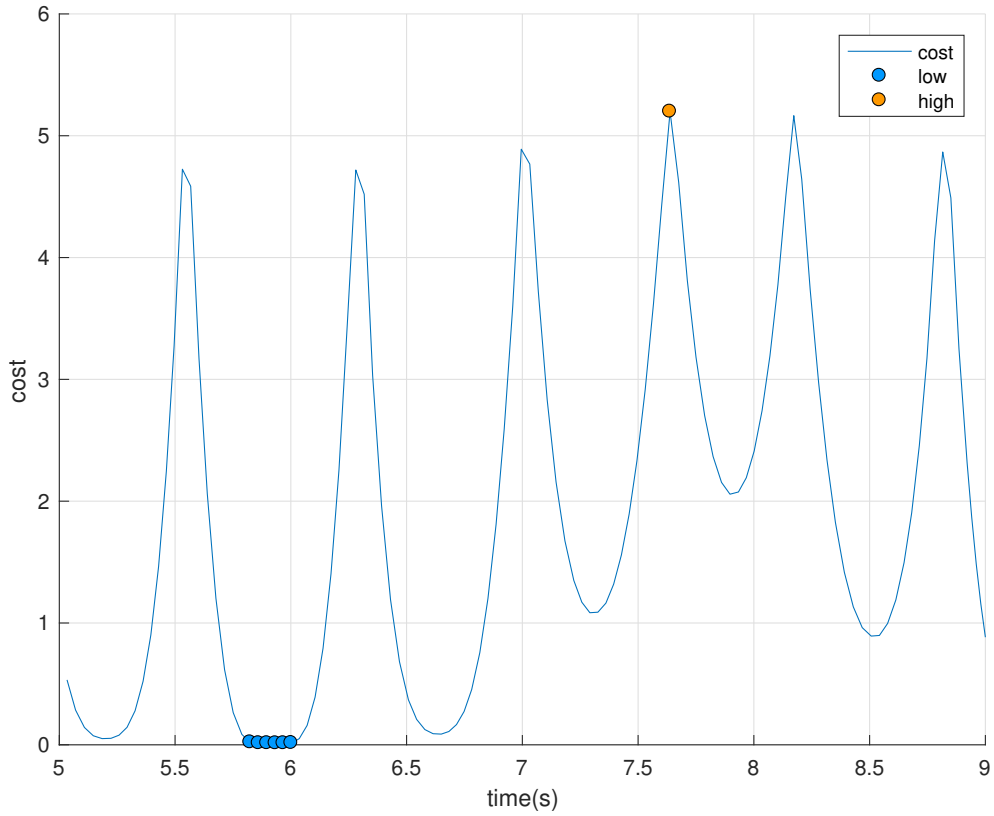

Figure 5.22: Minimum possible cost for every system state

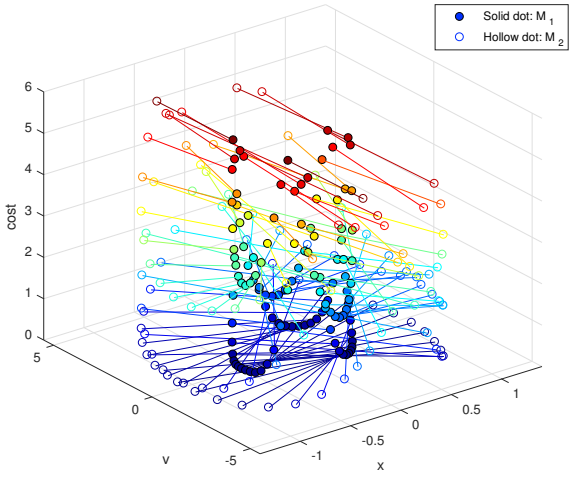

Figure 5.23: 3-D Phase-cost plot

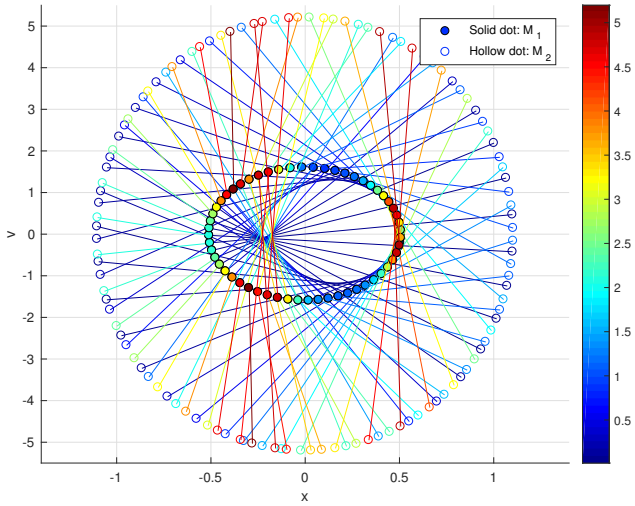

Figure 5.24: 3-D Phase-cost plot - top

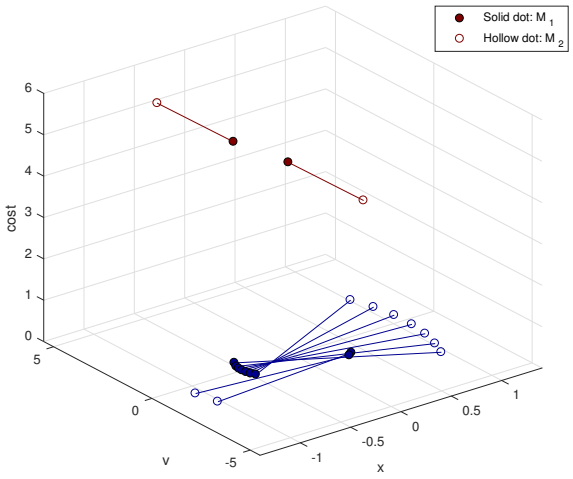

Figure 5.25: Extreme phase cases

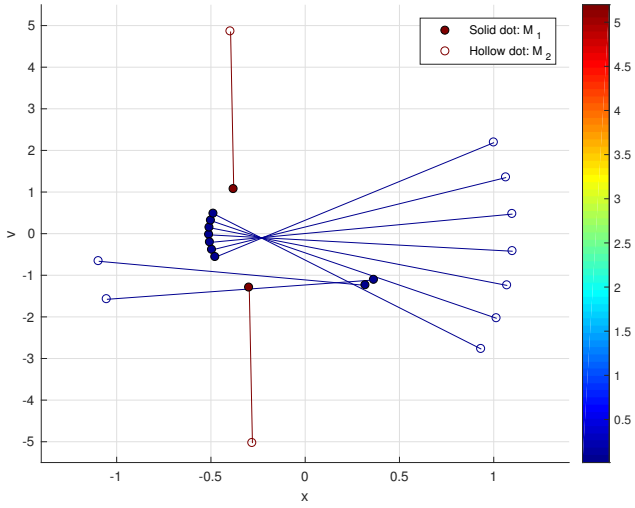

Figure 5.26: Extreme phase cases - top view

case 2-2: $\phi = \frac{\pi}{4}$

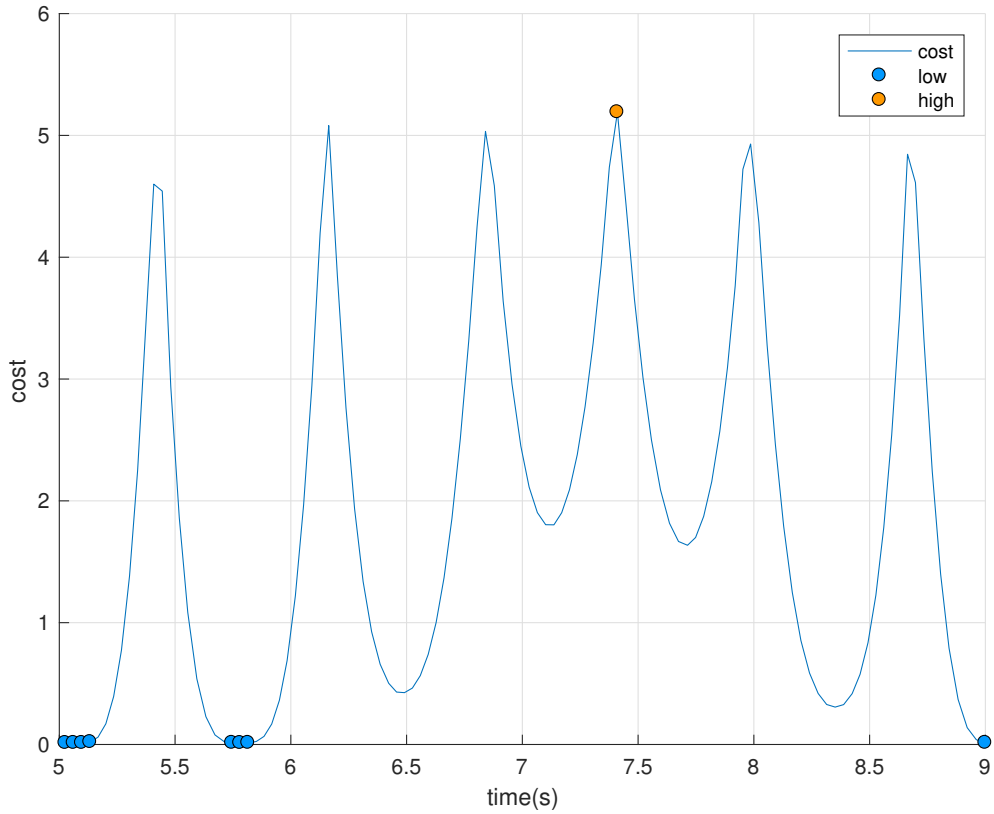

Figure 5.27: Minimum possible cost for every system state

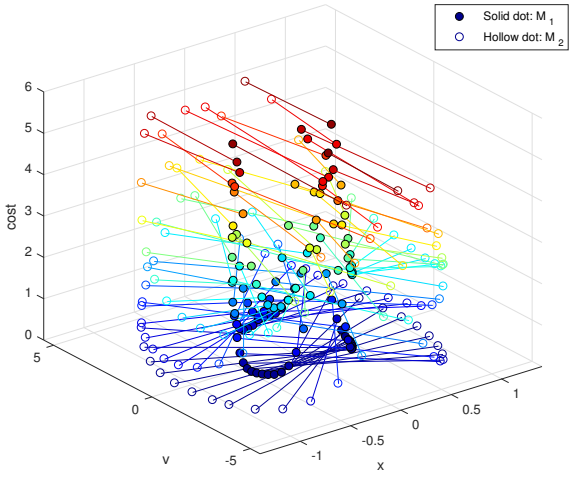

Figure 5.28: 3-D Phase-cost plot

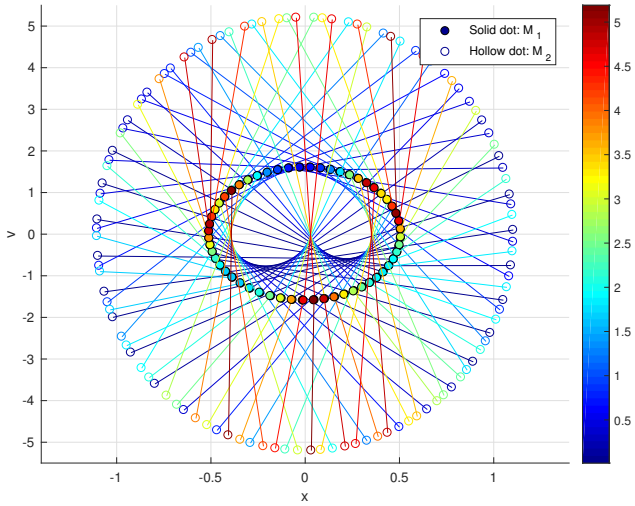

Figure 5.29: 3-D Phase-cost plot - top plan

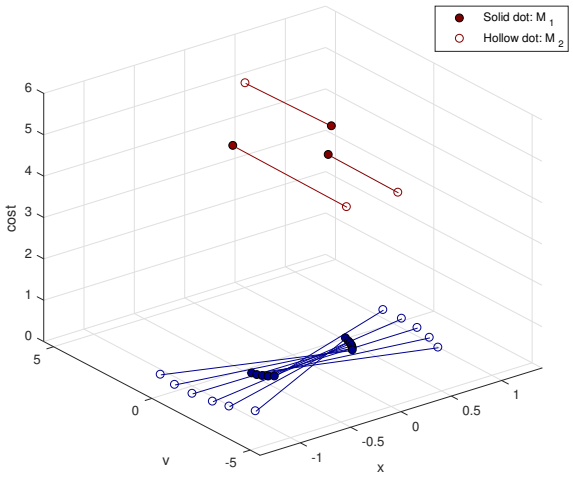

Figure 5.30: Extreme phase cases

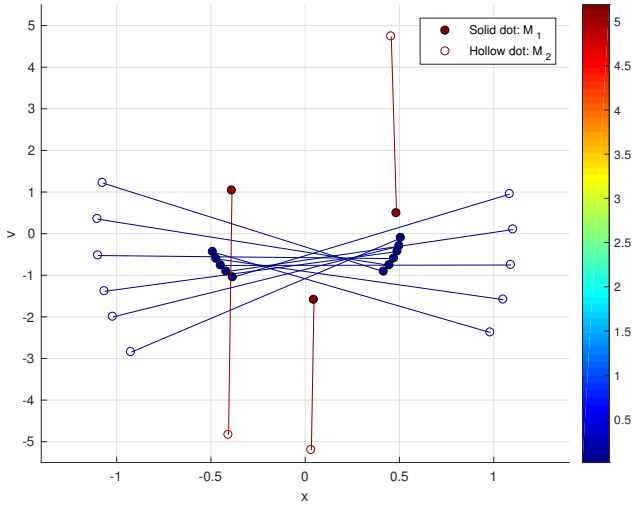

Figure 5.31: Extreme phase cases - top view

case 2-3: $\phi = \frac{\pi}{2}$

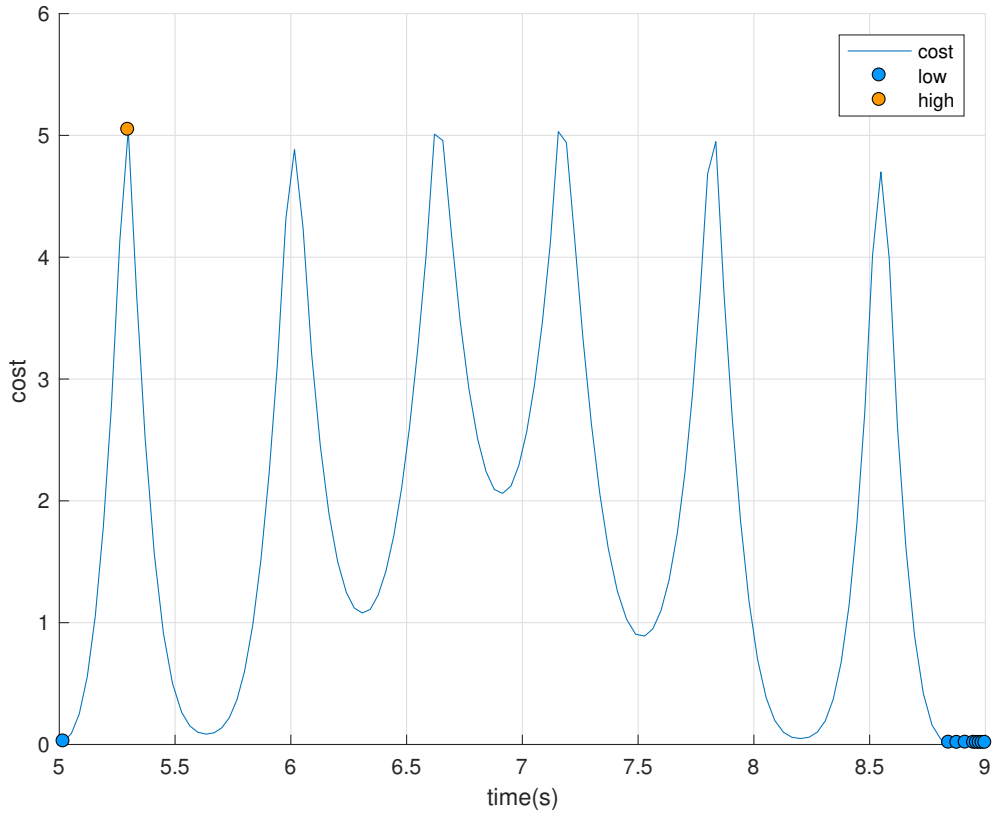

Figure 5.32: Minimum possible cost for every system state

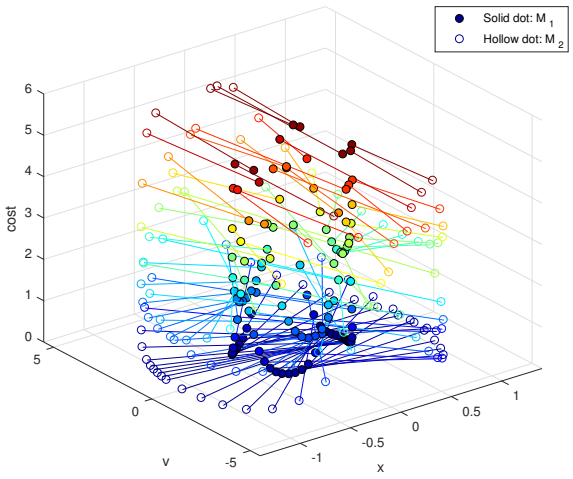

Figure 5.33: 3-D Phase-cost plot

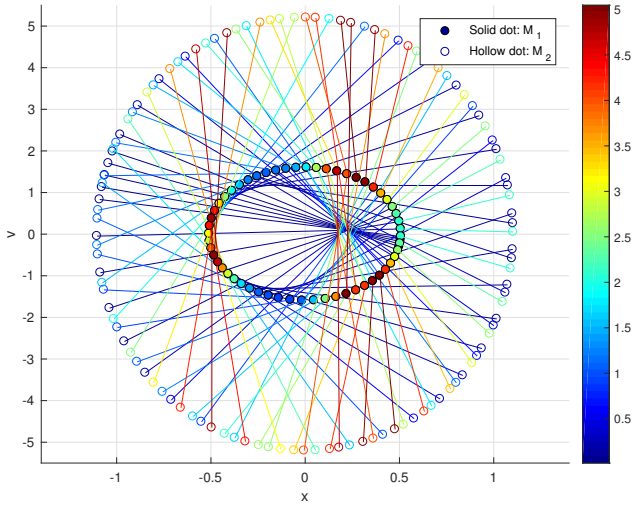

Figure 5.34: 3-D Phase-cost plot - top plan

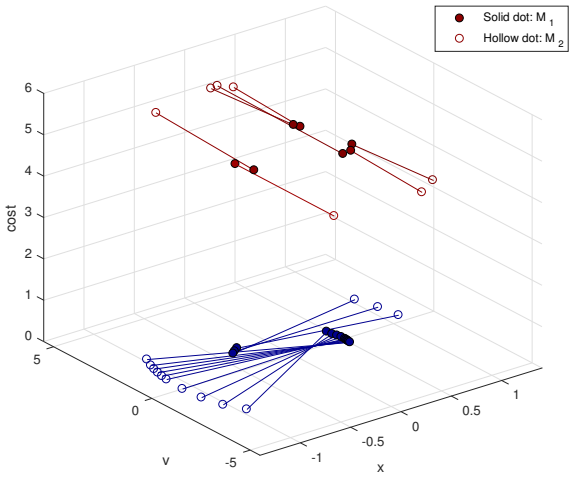

Figure 5.35: Extreme phase cases

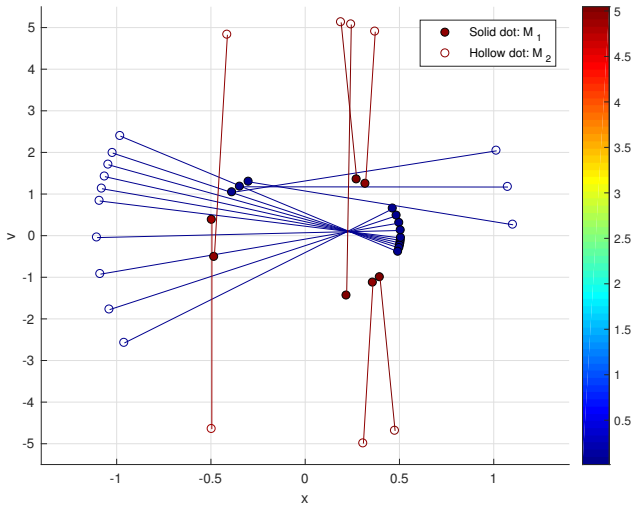

Figure 5.36: Extreme phase cases - top view

case 2-4: $\phi = \frac{3\pi}{4}$

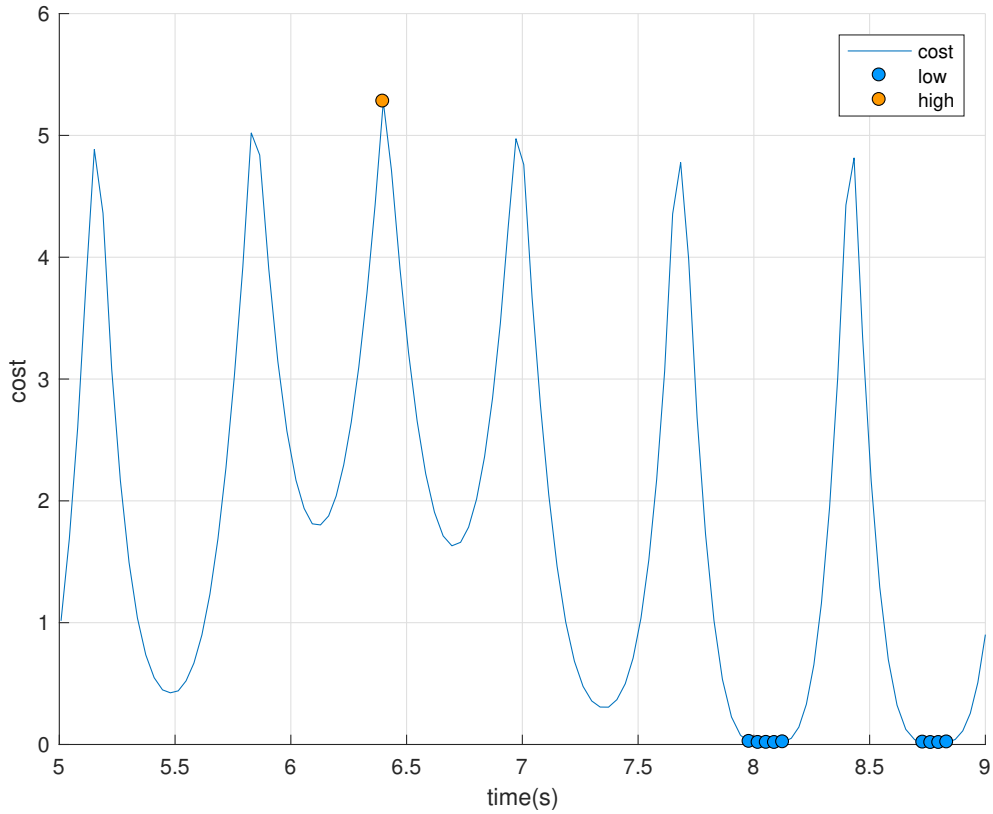

Figure 5.37: Minimum possible cost for every system state

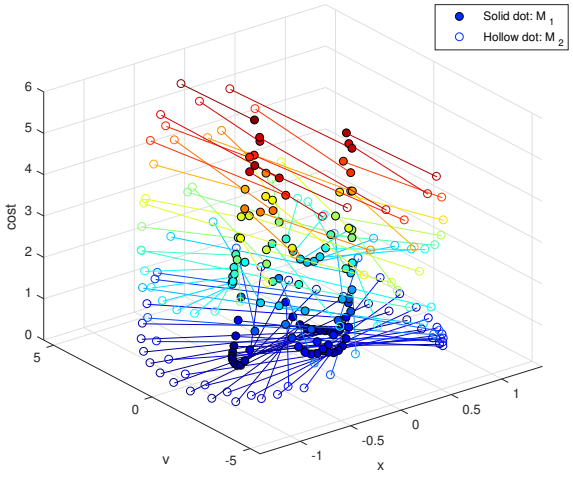

Figure 5.38: 3-D Phase-cost plot

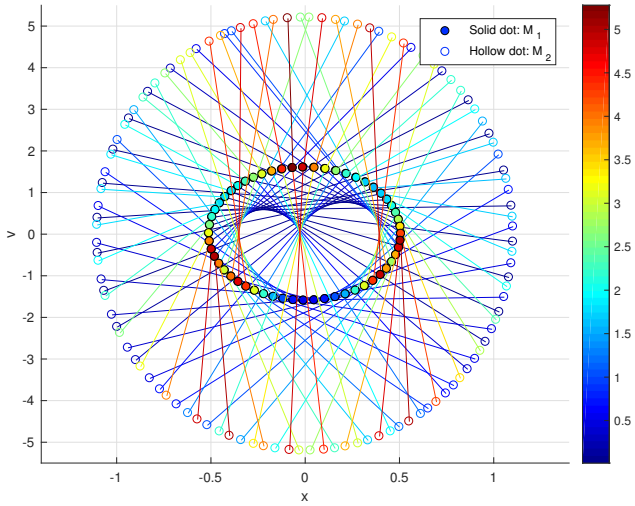

Figure 5.39: 3-D Phase-cost plot - top plan

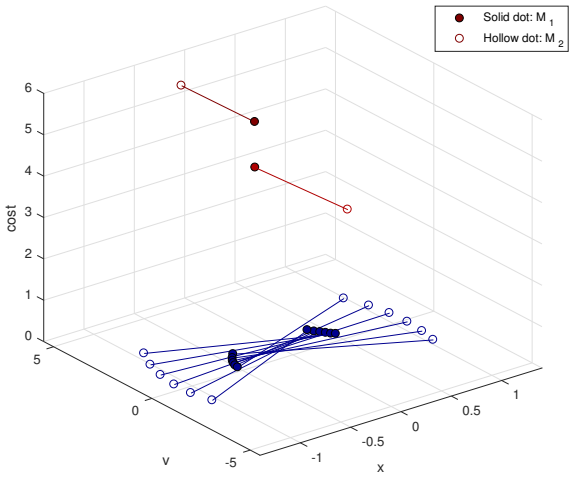

Figure 5.40: Extreme phase cases

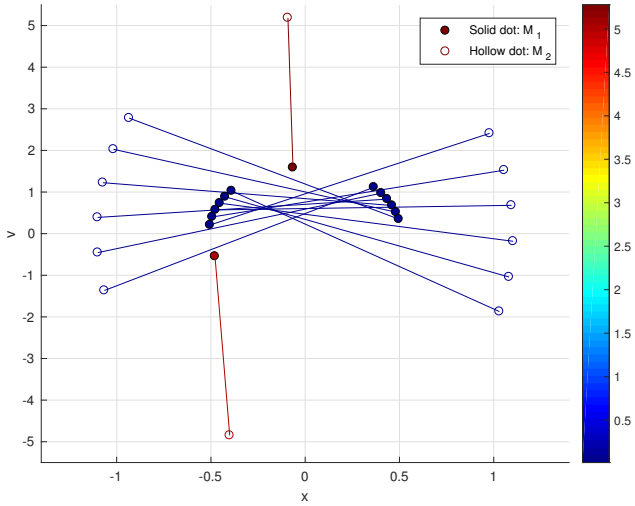

Figure 5.41: Extreme phase cases - top view

case 2-5: $\phi = \pi$

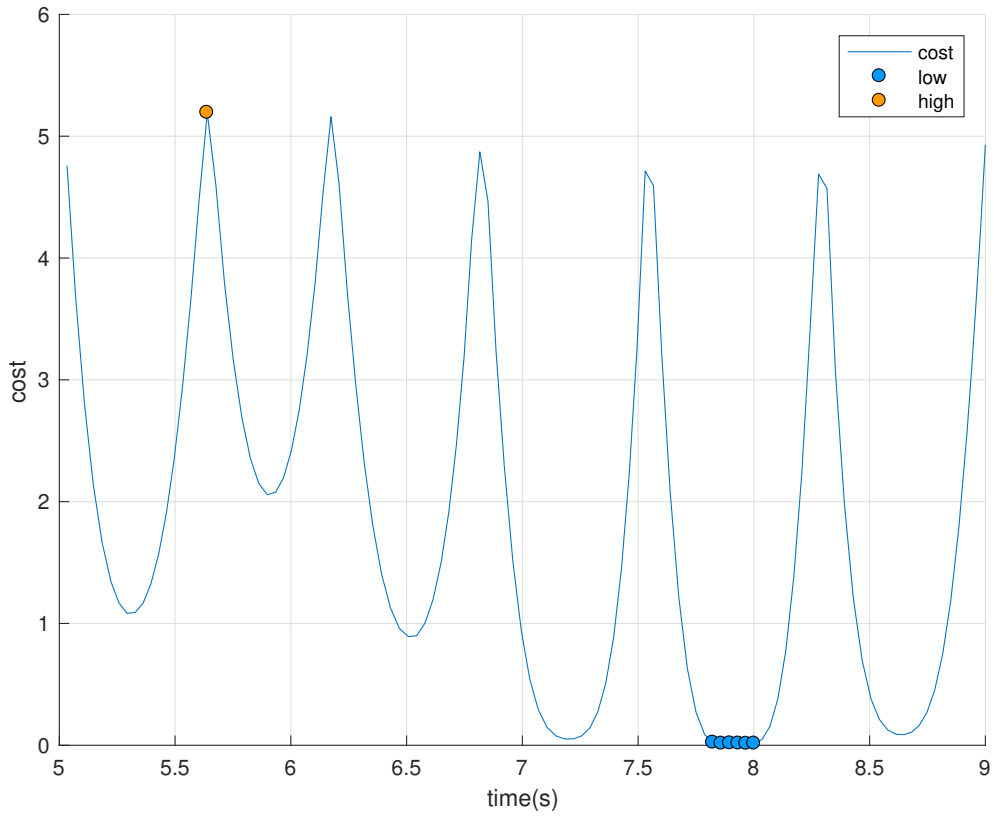

Figure 5.42: Minimum possible cost for every system state

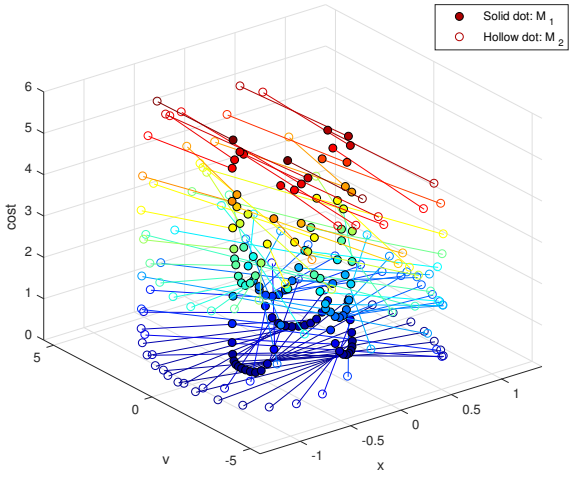

Figure 5.43: 3-D Phase-cost plot

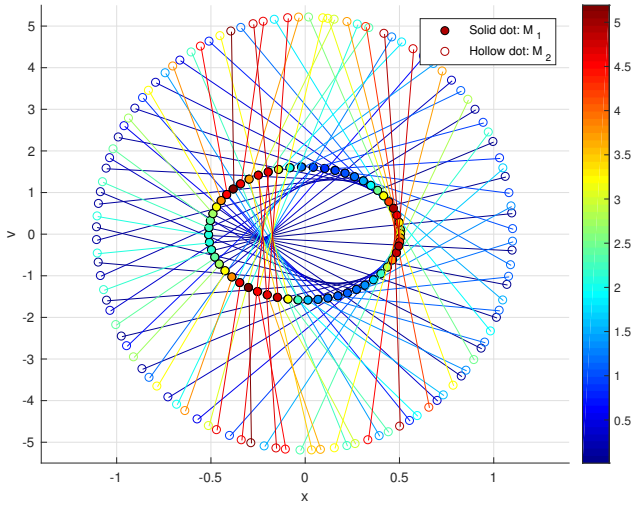

Figure 5.44: 3-D Phase-cost plot - top plan

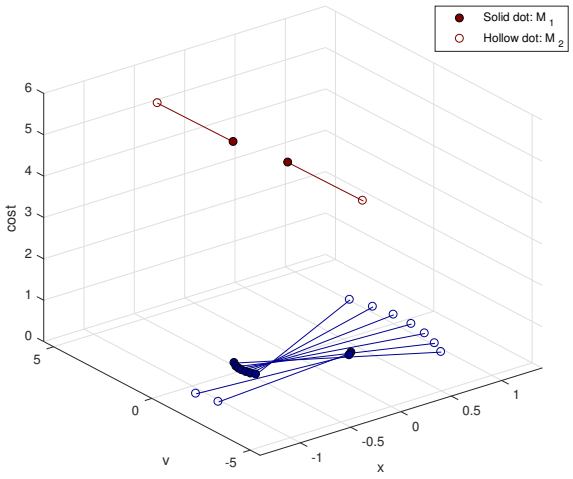

Figure 5.45: Extreme phase cases

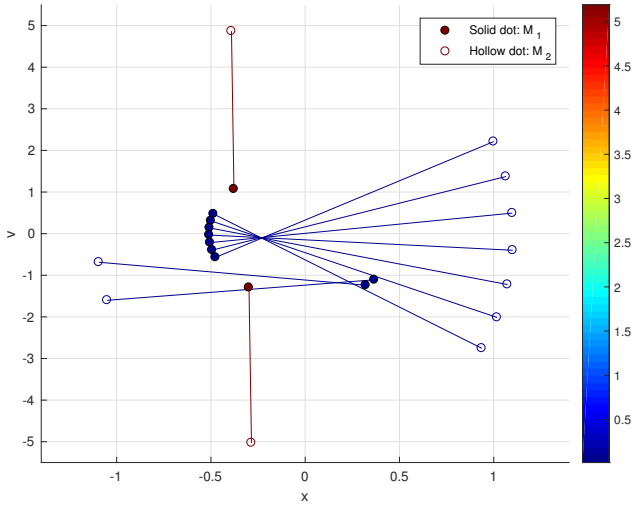

Figure 5.46: Extreme phase cases - top view

5.4 Summary of switching condition

From case study 1 we conclude that, the latch should be turned on whenever the velocity of M_1 and M_2 are almost the same for cases with forcing frequency not a lot greater than the highest natural frequency of the subsystems. In other words, to minimize the final cost, we should choose this condition to be the latch turn-on condition (C_{on}) in the control process in fig.(3.2).
On the otherhand, case study 2 shows that changes of phase angle of external force does not affect much on the relationship between final cost and the states. The conclusion made from case study 1 still valid even the system is being excited by forces with different phase angle.

Chapter 6

Real-time control

In chapter 5, we have found the condition for the latch whenever the velocity of two masses are the same in order to minimize the energy in M_1. With this revealation, we can now construct a control law to apply it in the simulations.

6.1 Control law

First in stage S1, we wait for a specific time period τ_s to get rid of the transient behavior of the system. After τ_s the system go into stage S2. If states achieved the turn-on condition C_{on} in S2, the system go into stage S3. Otherwise, the system stay at this stage until the condition is fullfilled. In stage S3, the latch is being turned on and the controller go right into next stage S4. In stage S4, the control algorithm wait for the condition C_{off} being satisfied to go into S5. The latch then being tuned off in stage S5. Finally, the controller evaluate the energy in M_1. If the energy is larger than arbitrary threshold E_{M1}, the controller return to the first stage and redo the whole process. We show our control law in the form of finite state machine.

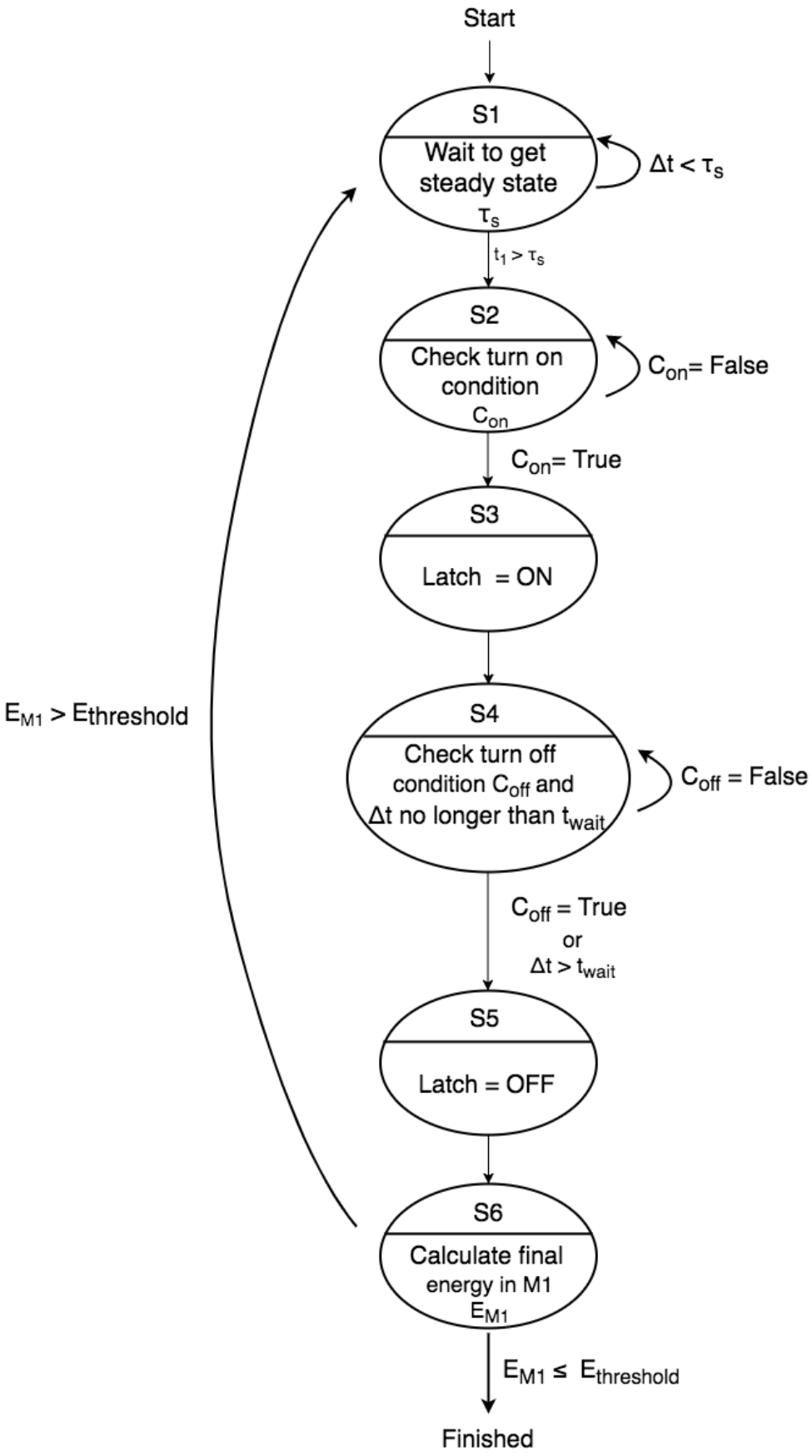

Figure 6.1: Finite state machine of control law

S1. Wait for the subsystem M_2 to go into steady state.

S2. Check for the turn on condition (C_{on})

S3. Turn on the latch.

S4. Check for turn off condition (C_{off}) within $\Delta t <= t_{wait}$.

S5. Turn off the latch

S6. Check the amount of energy E_{M1} in M_1.

6.2 Plots and results

We examine cases of different frequency of external force with the following system parameters and initial conditions,

$$\text{Initial condition} = \begin{cases} x_1(0) = -0.5 \\ x_2(0) = 0 \\ v_1(0) = 0.2 \\ v_2(0) = 0 \end{cases}, \qquad \begin{cases} w_{M_1} = 1.0\pi \\ w_{M_2} = 1.4\pi \end{cases} \tag{6.1}$$

6.2.1 Frequency under w_{M1} and w_{M2}

case1: $w_f = 0.2\pi$

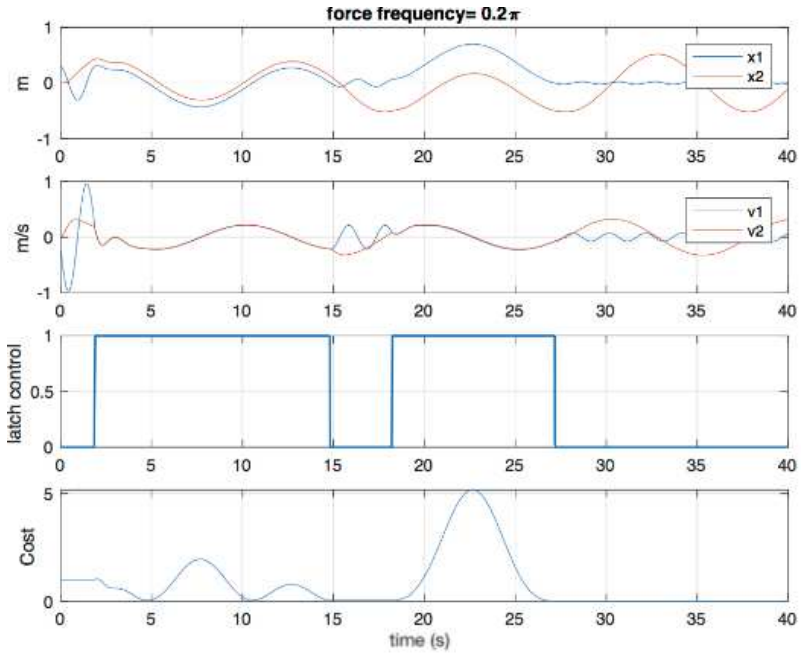

Figure 6.2: Time-domain simulation for $w_f = 0.2\pi$

case2: $w_f = 0.4\pi$

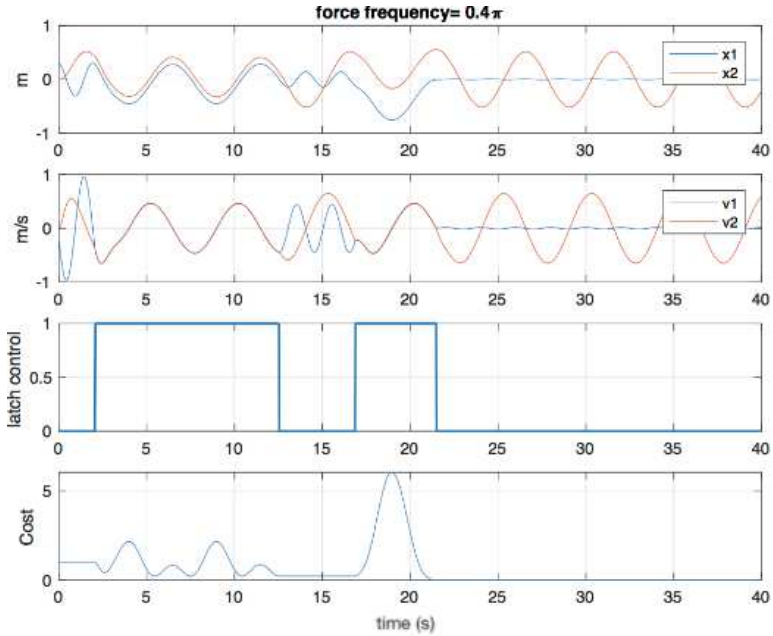

Figure 6.3: Time-domain simulation for $w_f = 0.4\pi$

case3: $w_f = 0.6\pi$

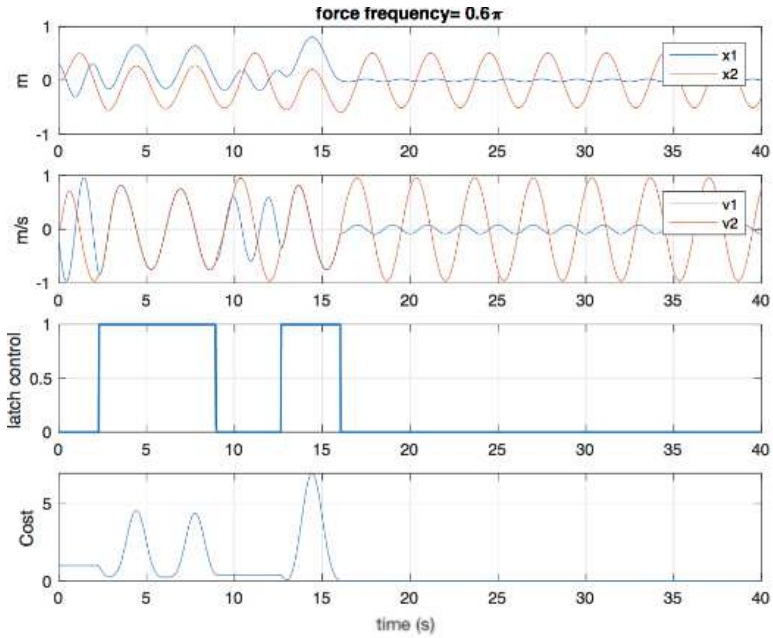

Figure 6.4: Time-domain simulation for $w_f = 0.6\pi$

case4: $w_f = 0.8\pi$

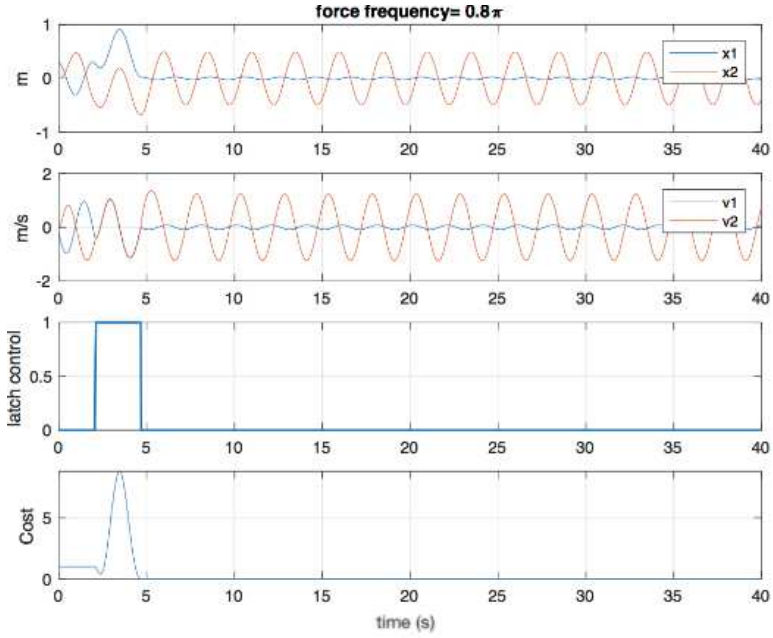

Figure 6.5: Time-domain simulation for $w_f = 0.8\pi$

case5: $w_f = 1.0\pi$

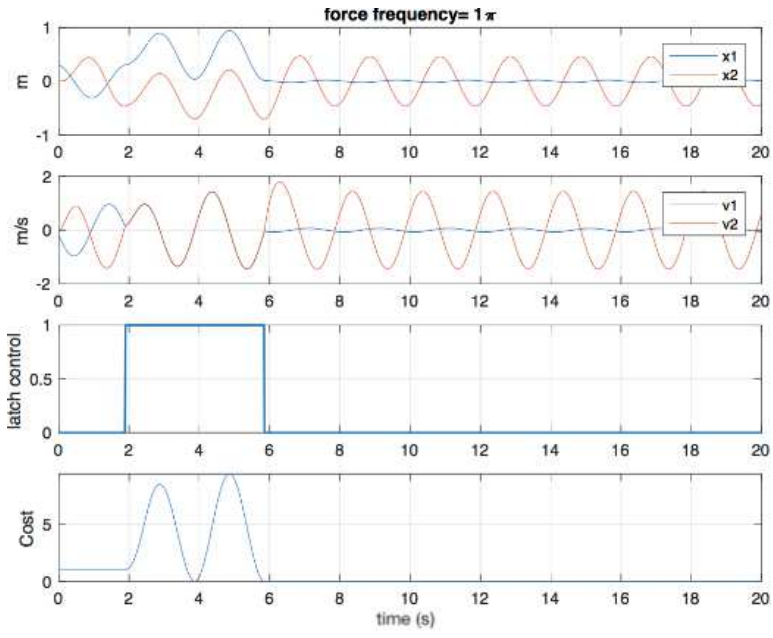

Figure 6.6: Time-domain simulation for $w_f = 1.0\pi$

case6: $w_f = 1.2\pi$

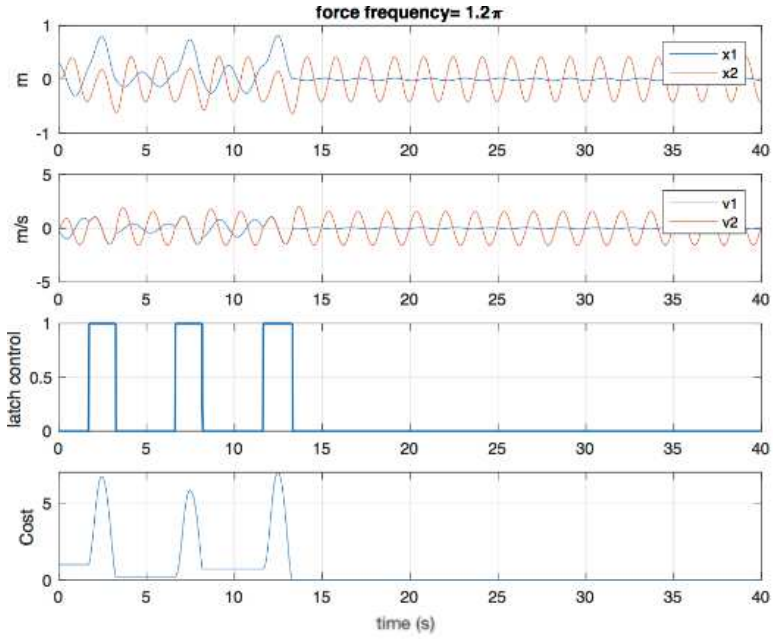

Figure 6.7: Time-domain simulation for $w_f = 1.2\pi$

case7: $w_f = 1.4\pi$

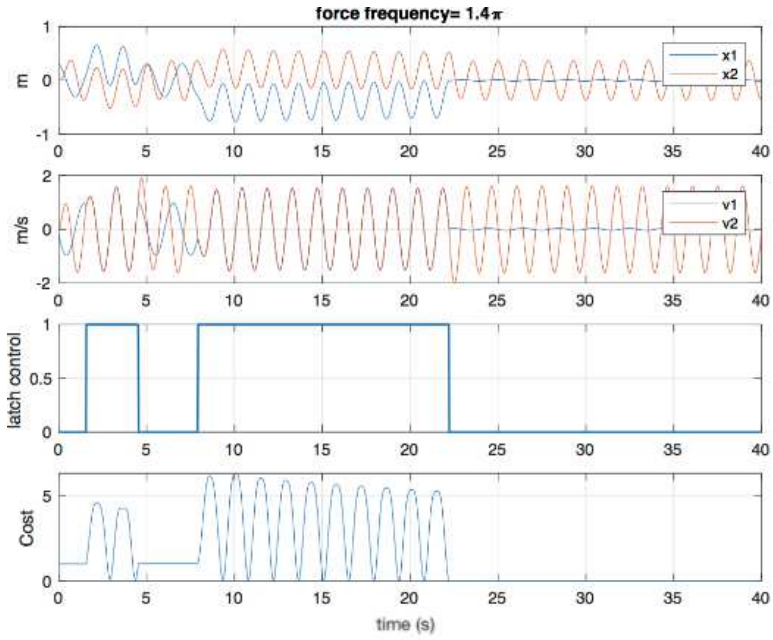

Figure 6.8: Time-domain simulation for $w_f = 1.4\pi$

6.2.2 Frequency over w_{M1} and w_{M2}

case8: $w_f = 1.5\pi$

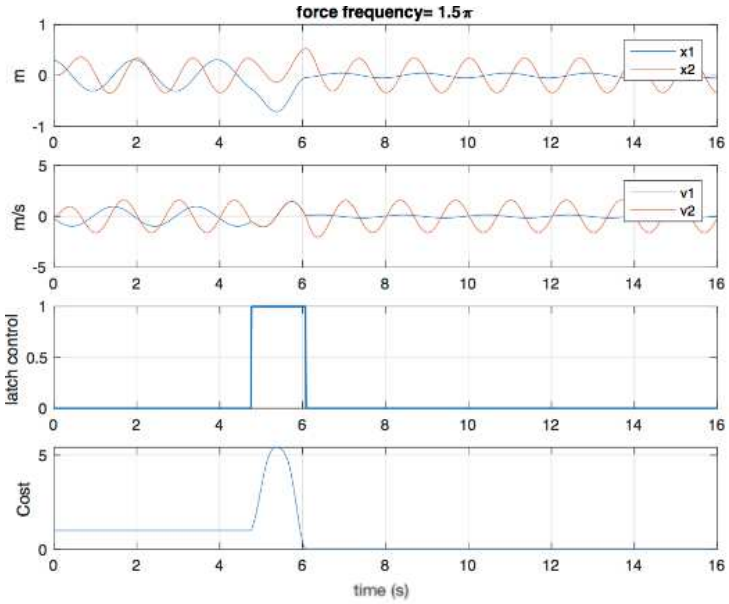

Figure 6.9: Time-domain simulation for $w_f = 1.5\pi$

case9: $w_f = 1.6\pi$

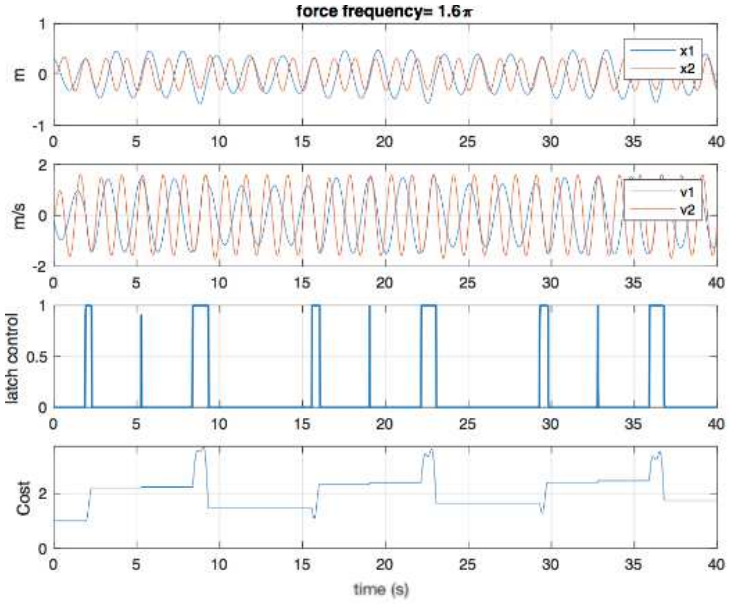

Figure 6.10: Time-domain simulation for $w_f = 1.6\pi$

case10: $w_f = 1.8\pi$

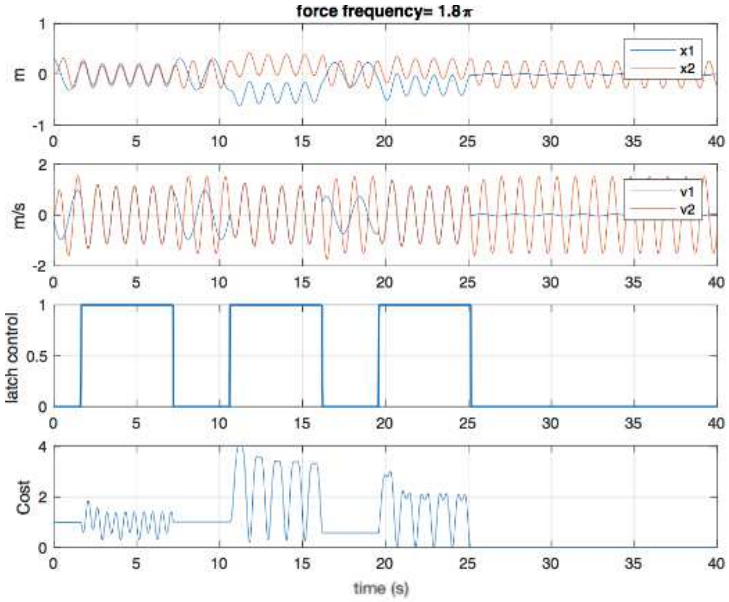

Figure 6.11: Time-domain simulation for $w_f = 1.8\pi$

6.2.3 Without external force

case11: No external force

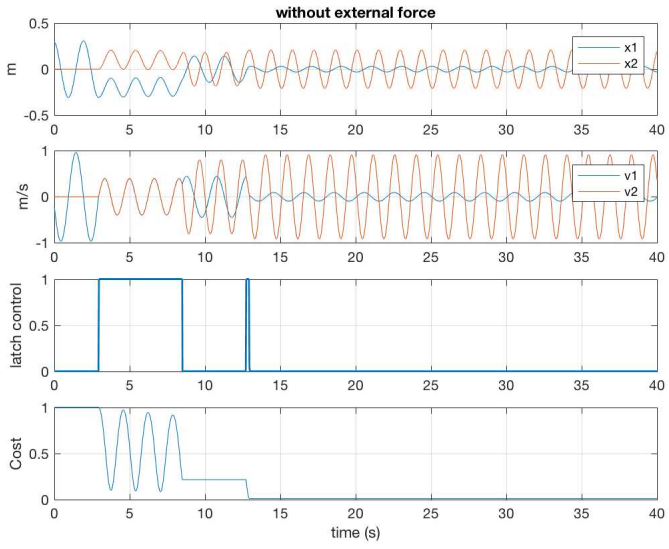

Figure 6.12: Time-domain simulation for $F_A = 0$

6.2.4 Observation

From the examples above, we noticed when w_f is smaller than the highest natural frequency within two subsystem, the control algorithm is capable to decrease the energy in M_1. However, it can also be observed that, the energy in M_1 is not strictly decreasing. It may increasing in the beginning but decreasing afterwards. Nevertheless, since there is no active device in the system, the maximum amount of energy in M_1 is bounded by the external perturbation. The system will not become unstable.
In case8 and case10, even though $w_f \geq w_{M2}$ the control algorithm is still capable to reduce the energy in M_1. However, the control algorithm is not applicable in the case9 which the forcing frequency is higher than than w_{M2}. In case11, we apply our real-time control law on the system we have discussed in the third chapter fig.(3.1). You can clearly see that the energy in M_1 is being transfered to M_2. It is an explicit evidence that the latch device is capable of redistributing energy in a dynamic system.

Chapter 7

Summary

7.1 Conclusions

From previous chapters we make the following conclusion,

- The latch element with proper control law is capable of redirecting energy in a dynamic structure.
- By examining the relationship betwen the cost and states, we deduced that when the velocity of both two masses are the same, it is the switch-on condition for the control law. This control law is applicable under the condition that the frequency of external force is not alot greater than the highest natural frequencies within two subsystems. Regarding to the condition for switch-off control law, we derived the latch should be turned off whenever the position and velocity is the closest to zero.
- To derived the analytic solution, we first consider a system without excitation. After we showed existence of the analytic solution for ideal case, the nonideal control law has been proposed. And we found that the real-time control law is valid for both excited and not excited systems.

7.2 Recommendation of future

We had demonstrated the possibility of latch device to redirect the energy in the system. Here, we provide a promising application for further research of the latch device. Since our real-time control law is very simple, FPGA (Field-Programmable Gate Array) is capable of not only developing sensors for detecting the event for switching condition but also controlling the latch. By connected several latches together and controlled by FPGA, it forms a multi-agent network with lots of degrees of freedom. With this flexibility in direction, the latches

in the network have the potential ability to redirect the in-flow vibration and to mitigate the energy directly going through the system. Furthermore, if directing the energy at our disposal is possible, we can acculmulate it for the later use for energy harvesting by adding in a energy harvesting devices into the networks, such as the energy-harvesting shock absorber [30] developed by Li, and Zuo et al.. That is to say, we don't need to amplify the minute voltage converted from ambient vibration to harvest energy effectively. Also, without voltage amplifier, the overall size of energy harvesting devices become smaller, and thus gain more compatibility in nonideal situations such as cramped environments.

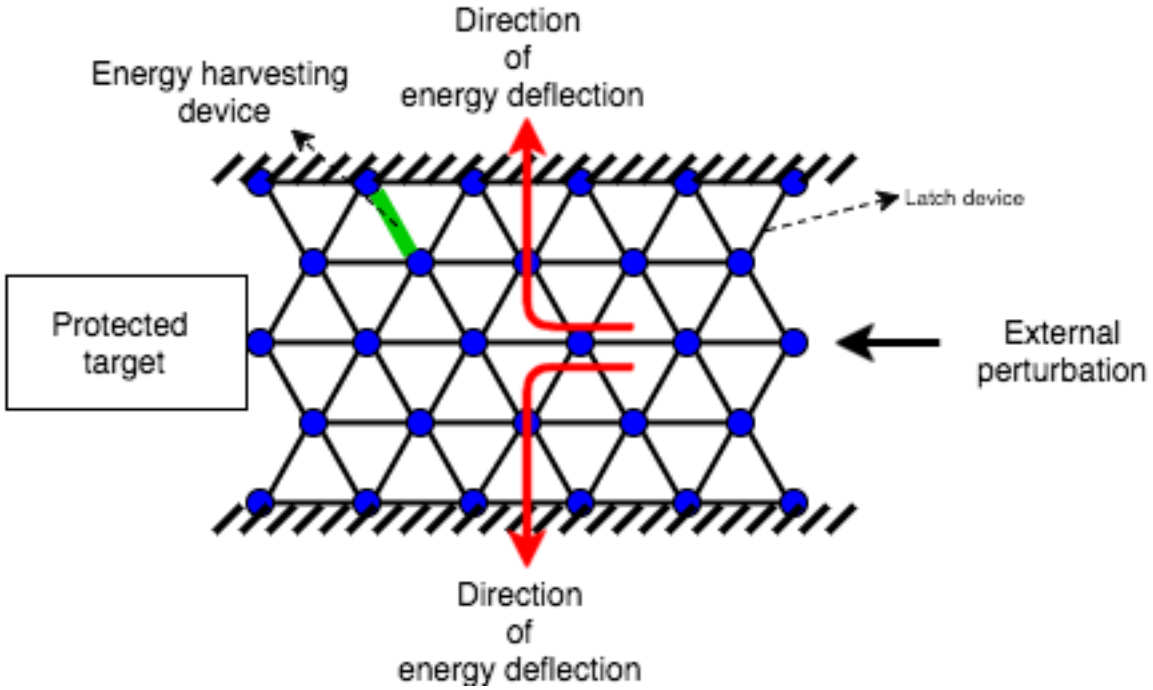

Figure 7.1: Potential application of multi-agent network of latch device

Bibliography

Bibliography

[1] Emelyanov, S.V. (1957). Method of designing complex control algorithms using an error and its first time-derivative only, Automation and Remote Control, 18(10) (In Russian)

[2] Hung JY, Gao W, Hung JC. Variable structure control: a survey. IEEE Transactions on Industrial Electronics. 1993;40(1):2-22.

[3] Shtessel, Yuri, et al. Sliding mode control and observation. Springer New York, 2014.

[4] Landau, Ioan Dor, et al. Adaptive ctrol: algorithms, analysis and applications. Springer Science & Business Media, 2011.

[5] Yu, Xinghuo, and Jian-Xin Xu, eds. Variable structure systems: towards the 21st century. Vol. 274. Springer Science & Business Media, 2002.

[6] Bartolini, Giorgio, et al. "On second order sliding mode controllers." Variable structure systems, sliding mode and nonlinear control. Springer Lond, 1999. 329-350.

[7] Edwards, Christopher, Enric Fossas Colet, and Leonid Fridman. Advances in variable structure and sliding mode control. Springer Verlag, 2006.

[8] J. -. E. Slotine and W. Li. Applied Nonlinear Control 1991.

[9] V. I. Utkin and SpringerLink (Online service). Sliding Modes in Control and Optimization 1992.

[10] K. D. Young, V. I. Utkin and U. Ozguner. A control engineer's guide to sliding mode control. IEEE Transactions on Control Systems Technology 7(3), pp. 328-342. 1999. . DOI: 10.1109/87.761053.

[11] M. B. dos Santos et al. Assessment of semi-active friction dampers. Mechanical Systems and Signal Processing 94pp. 33-56. 2017. . DOI: 10.1016/j.ymssp.2017.02.034. Cancel

[12] J. PardoVarela and J. C. Llera. A Semiactive piezoelectric friction damper. Earthquake Engineering & Structural Dynamics 44(3), pp. 333-354. 2015. . DOI: 10.1002/eqe.2469.

[13] T. F. FitzGerald et al. Slotted bolted connections in aseismic design for concentrically braced connections. Earthquake Spectra 5(2), pp. 383-391. 1989. . DOI: 10.1193/1.1585528.

[14] PALL, Avtar. Performance-based design using pall friction dampers-an economical design solution. In: 13th World Conference on Earthquake Engineering, Vancouver, BC, Canada. 2004.

[15] R. Zalewski et al. Dynamic model for a magnetorheological damper. Applied Mathematical Modelling 38(9-10), pp. 2366. 2014. . DOI: 10.1016/j.apm.2013.10.050.

[16] Bajkowski, J., et al. "A model for a magnetorheological damper." Mathematical and computer modelling 48.1 (2008): 56-68.

[17] Clegg, C. John. "A time-dependent nonlinear compensating network." Transactions of the American Institute of Electrical Engineers, Part II: Applications and Industry 75.5 (1956): 306-308.

[18] Garret, S. J. "Linear switching conditions for a third order positive-negative feedback control." Appl. Ind. 54 (1961).

[19] Emelyanov, S. V. "The use of nonlinear corrective devices of the key type to improve the behavior of second order control systems." Automatic Remote Control 7 (1959): 844-859.

[20] Flugge-Lotz, I., and C. Taylor. "Synthesis of a nonlinear control system." IRE transactions on automatic control 1.1 (1956): 3-9.

[21] Letov, A. M. "Conditionally stable control systems (on a class of optimal control systems)." Autom. Remote Control 18.7 (1957): 649-664.

[22] Emelyanov, S. V. "Theory of variable-structure control systems: Inception and initial development." Computational Mathematics and Modeling 18.4 (2007): 321-331.

[23] Spencer Jr, B. F., et al. "Phenomenological model for magnetorheological dampers." Journal of engineering mechanics 123.3 (1997): 230-238.

[24] Bergman LA, Spencer BF, Yao JTP, Masri SF, Skelton RE, Caughey TK, et al. Structural Control: Past, Present, and Future. Journal of Engineering Mechanics. 1997;123(9):897-971.

[25] S. Priya and D. J. Inman. Energy Harvesting Technologies 2009;2008;.

[26] S. V. Emelyanov, Variable Structure Control Systems. Moscow: Nauka (in Russian), 1967

[27] Y. Itkis, Control Systems of Variable Structure. New York: Wiley, 1976.

[28] G. N. Nikolski, On automatic stability of ship on given course, in Proc. Central Communication Lab.. no. I, pp. 34-75. 1934 (in Russian).

[29] Asai, T. (2014). Structural control strategies for earthquake response reduction of buildings (Order No. 3646439). Available from ProQuest Dissertations & Theses Global. (1639699276).

[30] Li, Zhongjie, et al. "Mechanical Motion Rectifier Based Energy-Harvesting Shock Absorber." ASME 2012 International Design Engineering Technical Conferences and Computers and Information in Engineering Conference. American Society of Mechanical Engineers, 2012.

[31] F. Nitzsche, A. Grewal, and D. Zimcik, inventors; Structural Component Having Means for Actively Varying its Stiffness to Control Vibrations, US patent 5,973,440, October 26, 1999.

[32] Yong, Chen, et al. "Development of the smart spring for active vibration control of helicopter blades." Journal of Intelligent Material Systems and Structures 15.1 (2004): 37-47.

[33] Larson, Gregg D. The analysis and realization of a state switched acoustic transducer. Diss. Georgia Institute of Technology, 1996.

[34] Clark, William W. "Semi-active vibration control with piezoelectric materials as variable-stiffness actuators." 1999 Symposium on Smart Structures and Materials. International Society for Optics and Photonics, 1999.

[35] Clark, William W. "Vibration control with state-switched piezoelectric materials." Journal of intelligent material systems and structures 11.4 (2000): 263-271.

[36] Corr, Lawrence R., and William W. Clark. "Comparison of low-frequency piezoceramic shunt techniques for structural damping." SPIE's 8th Annual International Symposium on Smart Structures and Materials. International Society for Optics and Photonics, 2001.

[37] Mickens, R. E. "A generalization of the method of harmonic balance." Journal of Sound and Vibration 111.3 (1986): 515-518.

[38] Mickens, R. E., and D. Semwogerere. "Fourier analysis of a rational harmonic balance approximation for periodic solutions." (1996): 528-550.

[39] Nitzsche, Fred, et al. "Development of a maximum energy extraction control for the smart spring." Journal of Intelligent Material Systems and Structures 16.11-12 (2005): 1057-1066.

[40] May, Jr William G. "Piezoelectric electromechanical translation apparatus." U.S. Patent No. 3,902,084. 26 Aug. 1975.

[41] Nishitani A, Nitta Y, Ishibashi Y. Structural control based on semi-active variable friction dampers. 12th WorldConference on Earthquake Engineering, Auckland, New Zealand, 2000.

Appendix: Analytic solution

$$
\begin{aligned}
&D_3(x_1(t), v_1(t), x_2(t), v_2(t)) = \\
&\frac{D_1^2 k_1^3}{(k_1+k_2)^2} - \frac{D_1^2 m_2^2 k_1^3}{(k_1+k_2)^2(m_1+m_2)^2} + \frac{2D_1 m_2^2 x_2 k_1^2}{(k_1+k_2)(m_1+m_2)^2} - \frac{2D_1^2 k_1^2}{k_1+k_2} + \frac{D_1^2 k_2 k_1^2}{(k_1+k_2)^2} + \frac{2LD_1 k_2 k_1^2}{(k_1+k_2)^2} - \frac{2D_1 D_2 k_2 k_1^2}{(k_1+k_2)^2} + \frac{2LD_1 m_2^2 k_1^2}{(k_1+k_2)(m_1+m_2)^2} - \\
&\frac{2D_1 D_2 m_2^2 k_1^2}{(k_1+k_2)(m_1+m_2)^2} - \frac{D_1^2 k_2 m_2^2 k_1^2}{(k_1+k_2)^2(m_1+m_2)^2} - \frac{2LD_1 k_2 m_2^2 k_1^2}{(k_1+k_2)^2(m_1+m_2)^2} + \frac{2D_1 D_2 k_2 m_2^2 k_1^2}{(k_1+k_2)^2(m_1+m_2)^2} + \frac{2D_1^2 m_1 m_2 k_1^2}{(k_1+k_2)(m_1+m_2)^2} + D_1^2 k_1 - \\
&\frac{m_2^2 x_2^2 k_1}{(m_1+m_2)^2} - \frac{2Lm_2^2 x_2 k_1}{(m_1+m_2)^2} + \frac{2D_2 m_2^2 x_2 k_1}{(m_1+m_2)^2} + \frac{2Lk_2 m_2^2 x_2 k_1}{(k_1+k_2)(m_1+m_2)^2} + \frac{2D_1 k_2 m_2^2 x_2 k_1}{(k_1+k_2)(m_1+m_2)^2} - \frac{2D_2 k_2 m_2^2 x_2 k_1}{(k_1+k_2)(m_1+m_2)^2} - \frac{2D_1 m_1 m_2 x_2 k_1}{(m_1+m_2)^2} - \\
&\frac{2D_1^2 k_2 k_1}{k_1+k_2} - \frac{2LD_1 k_2 k_1}{k_1+k_2} + \frac{2D_1 D_2 k_2 k_1}{k_1+k_2} + \frac{L^2 k_2^2 k_1}{(k_1+k_2)^2} + \frac{D_2^2 k_2^2 k_1}{(k_1+k_2)^2} + \frac{2LD_1 k_2^2 k_1}{(k_1+k_2)^2} - \frac{2LD_2 k_2^2 k_1}{(k_1+k_2)^2} - \frac{2D_1 D_2 k_2^2 k_1}{(k_1+k_2)^2} - \frac{D_1^2 m_1^2 k_1}{(m_1+m_2)^2} - \\
&\frac{L^2 m_2^2 k_1}{(m_1+m_2)^2} - \frac{D_2^2 m_2^2 k_1}{(m_1+m_2)^2} + \frac{2LD_2 m_2^2 k_1}{(m_1+m_2)^2} + \frac{2L^2 k_2 m_2^2 k_1}{(k_1+k_2)(m_1+m_2)^2} + \frac{2D_2^2 k_2 m_2^2 k_1}{(k_1+k_2)(m_1+m_2)^2} + \frac{2LD_1 k_2 m_2^2 k_1}{(k_1+k_2)(m_1+m_2)^2} - \frac{4LD_2 k_2 m_2^2 k_1}{(k_1+k_2)(m_1+m_2)^2} - \\
&\frac{2D_1 D_2 k_2 m_2^2 k_1}{(k_1+k_2)(m_1+m_2)^2} - \frac{L^2 k_2^2 m_2^2 k_1}{(k_1+k_2)^2(m_1+m_2)^2} - \frac{D_2^2 k_2^2 m_2^2 k_1}{(k_1+k_2)^2(m_1+m_2)^2} - \frac{2LD_1 k_2^2 m_2^2 k_1}{(k_1+k_2)^2(m_1+m_2)^2} + \frac{2LD_2 k_2^2 m_2^2 k_1}{(k_1+k_2)^2(m_1+m_2)^2} + \\
&\frac{2D_1 D_2 k_2^2 m_2^2 k_1}{(k_1+k_2)^2(m_1+m_2)^2} - \frac{2LD_1 m_1 m_2 k_1}{(m_1+m_2)^2} + \frac{2D_1 D_2 m_1 m_2 k_1}{(m_1+m_2)^2} + \frac{2D_1^2 k_2 m_1 m_2 k_1}{(k_1+k_2)(m_1+m_2)^2} + \frac{2LD_1 k_2 m_1 m_2 k_1}{(k_1+k_2)(m_1+m_2)^2} - \frac{2D_1 D_2 k_2 m_1 m_2 k_1}{(k_1+k_2)(m_1+m_2)^2} - \\
&\frac{m_1^2 v_1^2}{m_1+m_2} - \frac{m_2^2 v_2^2}{m_1+m_2} - \frac{k_2 m_2^2 x_2^2}{(m_1+m_2)^2} + D_1^2 k_2 + D_3^2 \left(\frac{k_2^3}{(k_1+k_2)^2} - \frac{m_2^2 k_2^3}{(k_1+k_2)^2(m_1+m_2)^2} + \frac{k_1 k_2^2}{(k_1+k_2)^2} + \right. \\
&\left. \frac{2m_2^2 k_2^2}{(k_1+k_2)(m_1+m_2)^2} - \frac{k_1 m_2^2 k_2^2}{(k_1+k_2)^2(m_1+m_2)^2} + \frac{2k_1 m_2^2 k_2}{(k_1+k_2)(m_1+m_2)^2} - \frac{m_2^2 k_2}{(m_1+m_2)^2} - \frac{k_1 m_2^2}{(m_1+m_2)^2} \right) - \frac{2m_1 m_2 v_1 v_2}{m_1+m_2} \\
&- \frac{2Lk_2 m_2^2 x_2}{(m_1+m_2)^2} + \frac{2D_2 k_2 m_2^2 x_2}{(m_1+m_2)^2} + \frac{2Lk_2^2 m_2^2 x_2}{(k_1+k_2)(m_1+m_2)^2} - \frac{2D_2 k_2^2 m_2^2 x_2}{(k_1+k_2)(m_1+m_2)^2} - \frac{2D_1 k_2 m_1 m_2 x_2}{(m_1+m_2)^2} + D_3 \left(-\frac{2Lk_2^3}{(k_1+k_2)^2} + \frac{2D_2 k_2^3}{(k_1+k_2)^2} + \right. \\
&\frac{2Lm_2^2 k_2^3}{(k_1+k_2)^2(m_1+m_2)^2} - \frac{2D_2 m_2^2 k_2^3}{(k_1+k_2)^2(m_1+m_2)^2} - \frac{2m_2^2 x_2 k_2^2}{(k_1+k_2)(m_1+m_2)^2} + \frac{2D_1 k_2^2}{k_1+k_2} - \frac{2Lk_1 k_2^2}{(k_1+k_2)^2} - \frac{2D_1 k_1 k_2^2}{(k_1+k_2)^2} + \frac{2D_2 k_1 k_2^2}{(k_1+k_2)^2} - \\
&\frac{4Lm_2^2 k_2^2}{(k_1+k_2)(m_1+m_2)^2} + \frac{4D_2 m_2^2 k_2^2}{(k_1+k_2)(m_1+m_2)^2} + \frac{2Lk_1 m_2^2 k_2^2}{(k_1+k_2)^2(m_1+m_2)^2} + \frac{2D_1 k_1 m_2^2 k_2^2}{(k_1+k_2)^2(m_1+m_2)^2} - \frac{2D_2 k_1 m_2^2 k_2^2}{(k_1+k_2)^2(m_1+m_2)^2} - \\
&\frac{2D_1 m_1 m_2 k_2^2}{(k_1+k_2)(m_1+m_2)^2} - \frac{2k_1 m_2^2 x_2 k_2}{(k_1+k_2)(m_1+m_2)^2} + \frac{2m_2^2 x_2 k_2}{(m_1+m_2)^2} + \frac{2D_1 k_1 k_2}{k_1+k_2} - \frac{2D_1 k_1^2 k_2}{(k_1+k_2)^2} + \frac{2Lm_2^2 k_2}{(m_1+m_2)^2} - \frac{2D_2 m_2^2 k_2}{(m_1+m_2)^2} - \\
&\frac{4Lk_1 m_2^2 k_2}{(k_1+k_2)(m_1+m_2)^2} - \frac{2D_1 k_1 m_2^2 k_2}{(k_1+k_2)(m_1+m_2)^2} + \frac{4D_2 k_1 m_2^2 k_2}{(k_1+k_2)(m_1+m_2)^2} + \frac{2D_1 k_1^2 m_2^2 k_2}{(k_1+k_2)^2(m_1+m_2)^2} + \frac{2D_1 m_1 m_2 k_2}{(m_1+m_2)^2} - \frac{2D_1 k_1 m_1 m_2 k_2}{(k_1+k_2)(m_1+m_2)^2} \\
&\left. + \frac{2k_1 m_2^2 x_2}{(m_1+m_2)^2} + \frac{2Lk_1 m_2^2}{(m_1+m_2)^2} - \frac{2D_2 k_1 m_2^2}{(m_1+m_2)^2} - \frac{2D_1 k_1^2 m_2^2}{(k_1+k_2)(m_1+m_2)^2} + \frac{2D_1 k_1 m_1 m_2}{(m_1+m_2)^2} \right) - \frac{2LD_1 k_2^2}{k_1+k_2} + \frac{2D_1 D_2 k_2^2}{k_1+k_2} + \frac{L^2 k_2^3}{(k_1+k_2)^2} + \\
&\frac{D_2^2 k_2^3}{(k_1+k_2)^2} - \frac{2LD_2 k_2^3}{(k_1+k_2)^2} - \frac{D_1^2 k_2 m_1^2}{(m_1+m_2)^2} - \frac{L^2 k_2 m_2^2}{(m_1+m_2)^2} - \frac{D_2^2 k_2 m_2^2}{(m_1+m_2)^2} + \frac{2LD_2 k_2 m_2^2}{(m_1+m_2)^2} + \frac{2L^2 k_2^2 m_2^2}{(k_1+k_2)(m_1+m_2)^2} + \frac{2D_2^2 k_2^2 m_2^2}{(k_1+k_2)(m_1+m_2)^2} - \\
&\frac{4LD_2 k_2^2 m_2^2}{(k_1+k_2)(m_1+m_2)^2} - \frac{L^2 k_2^3 m_2^2}{(k_1+k_2)^2(m_1+m_2)^2} - \frac{D_2^2 k_2^3 m_2^2}{(k_1+k_2)^2(m_1+m_2)^2} + \frac{2LD_2 k_2^3 m_2^2}{(k_1+k_2)^2(m_1+m_2)^2} - \frac{2LD_1 k_2 m_1 m_2}{(m_1+m_2)^2} + \frac{2D_1 D_2 k_2 m_1 m_2}{(m_1+m_2)^2} + \\
&\frac{2LD_1 k_2^2 m_1 m_2}{(k_1+k_2)(m_1+m_2)^2} - \frac{2D_1 D_2 k_2^2 m_1 m_2}{(k_1+k_2)(m_1+m_2)^2}
\end{aligned}
$$